10-2018

Impact of Seabed Resuspension on Oxygen and Nitrogen Dynamics in the Northern Gulf of Mexico: A Numerical Modeling Study

Julia M. Moriarty
Virginia Institute of Marine Science

Courtney K. Harris
Virginia Institute of Marine Science

Marjorie A.M. Friedrichs
Virginia Institute of Marine Science

Katja Fennel

Kehui Xu

Recommended Citation

RESEARCH ARTICLE

Key Points:
- A hydrodynamic-sediment transport-biogeochemical model shows that resuspension exacerbates hypoxia in the northern Gulf of Mexico
- Resuspension of seabed organic matter intensifies water column remineralization, increasing oxygen consumption and ammonium production
- Effects of resuspension are largest in regions with abundant seabed particulate organic matter that is subject to frequent resuspension

Impact of Seabed Resuspension on Oxygen and Nitrogen Dynamics in the Northern Gulf of Mexico: A Numerical Modeling Study

Julia M. Moriarty[1,2] [iD]**, Courtney K. Harris[1]** [iD]**, Marjorie A. M. Friedrichs[1]** [iD]**, Katja Fennel[3]** [iD]**, and Kehui Xu[4,5]**

[1]Virginia Institute of Marine Science, College of William and Mary, Gloucester Point, Gloucester, VA, USA, [2]Now at U.S. Geological Survey, Woods Hole, MA, USA, [3]Department of Oceanography, Dalhousie University, Halifax, Nova Scotia, Canada, [4]Department of Oceanography and Coastal Sciences, Louisiana State University, Baton Rouge, LA, USA, [5]Coastal Studies Institute, Louisiana State University, Baton Rouge, LA, USA

Abstract Resuspension affects water quality in coastal environments by entraining seabed organic matter into the water column, which can increase remineralization, alter seabed fluxes, decrease water clarity, and affect oxygen and nutrient dynamics. Nearly all numerical models of water column biogeochemistry, however, simplify seabed and bottom boundary layer processes and neglect resuspension. Here we implemented HydroBioSed, a coupled hydrodynamic-sediment transport-biogeochemical model to examine the role of resuspension in regulating oxygen and nitrogen dynamics on timescales of a day to a month. The model was implemented for the northern Gulf of Mexico, where the extent of summertime hypoxia is sensitive to seabed and bottom boundary layer processes. Results indicated that particulate organic matter remineralization in the bottom water column increased by an order of magnitude during resuspension events. This increased sediment oxygen consumption and ammonium production, which were defined as the sum of seabed fluxes of oxygen and ammonium, plus oxygen consumption and ammonium production in the water column due to resuspended organic matter. The increases in remineralization impacted biogeochemical dynamics to a greater extent than resuspension-induced seabed fluxes and oxidation of reduced chemical species. The effect of resuspension on bottom water biogeochemistry increased with particulate organic matter availability, which was modulated by sediment transport patterns. Overall, when averaged over the shelf and on timescales of a month in the numerical model, cycles of erosion and deposition accounted for about two thirds of sediment oxygen consumption and almost all of the sediment ammonium production.

Plain Language Summary In coastal waters, oxygen and nitrogen levels affect the health of fish and other organisms. In the Gulf of Mexico, for example, low-oxygen regions called hypoxic areas or "dead zones" form in the summertime near the seabed in "bottom water". It can be difficult to understand and quantify variations in bottom water oxygen and nitrogen levels, however, because: (1) water quality there is affected by many different physical and biological processes; and (2) observational studies are limited by cost, safety and technological advances. To complement previous observational studies, this paper used a new numerical modeling approach that accounts for many physical and biological processes in the seabed and water. Specifically, we used the model to evaluate how resuspension, especially the entrainment of organic matter from the seabed into the water, affected oxygen and nitrogen levels in the Northern Gulf of Mexico. Model results indicated that resuspension increased the decomposition of organic matter, decreasing oxygen levels and increasing ammonium (a form of nitrogen) levels in bottom water. This effect was largest in regions with abundant seabed organic matter and frequent resuspension. These modeling results can help scientists and environmental managers understand how resuspension affects oxygen and nitrogen levels in bottom waters.

1. Introduction

Biogeochemical cycles and water quality in coastal waters are modulated by processes in the seabed and bottom boundary layer, defined as the near-bed region of the water column (Aller, 1998; McKee et al., 2004; see Table 1 for definitions). These processes, such as organic matter remineralization and seabed-water column fluxes, are affected by various physical and biogeochemical factors, complicating our ability to understand and quantify them, as well as their ability to modulate coastal water quality (e.g., Conley et al., 2009; Connolly et al., 2010) and ecosystem response to management efforts (Kemp et al., 2009). For example,

Table 1
*Description of Phrases, Acronyms, and Abbreviations, as Used in This Paper*

Acronym/abbreviation	Description
Bottom boundary layer	The region of the water column above the seabed where friction from the seabed affects fluid flow that is typically meters in thickness (Grant & Madsen,1986; Nielsen, 1992). This definition differs from an alternate definition, that the bottom or benthic boundary layer includes the surficial seabed and bottom water column (Boudreau & Jorgensen, 2001; McKee et al., 2004).
Bottom water	The region of the water column within 1 m of the seabed where suspended sediment concentrations were high during resuspension events.
CSTMS	Community Sediment Transport Modeling System.
Effective remineralization rate	See remineralization.
HydroBioSed	The coupled hydrodynamic-sediment transport-water column and seabed biogeochemistry used in this study.
Module	Refers to a submodel within a model, for example, the sediment transport module within ROMS.
Nudging	A simple form of data assimilation used in numerical models. In the context of this manuscript, model estimates were replaced with a weighted average of the original model estimate and an observed value.
POC	Particulate organic carbon.
POM	Particulate organic matter.
Quasi one-dimensional model	A multidimensional model that is implemented as a one-dimensional model. For example, Moriarty et al. (2017) used a small horizontal grid and periodic boundary conditions so that conditions were horizontally uniform and only varied in the vertical dimension.
Remineralization	Refers to the temporal rate of change in POC concentrations due to decomposition, with a unit of carbon concentration $* \text{time}^{-1}$.
Remineralization rate constant	A temporally and spatially constant model parameter with units of inverse time that characterizes organic matter decomposition.
ROMS	Regional Ocean Modeling System.
Seabed	Region beneath the water column and bottom boundary layer.
Seabed oxygen consumption	Oxygen consumption that occurs within the seabed, not in the water column or bottom boundary layer.
Sediment	Inorganic (i.e., mineral) particles.
Sediment ammonium production	**Total ammonium production** has three components: (1) the net flux of ammonium out of the seabed, (2) water column ammonium production due to remineralization of resuspended POM, and (3) water column ammonium production due to remineralization of non-resuspended POM. **Sediment ammonium production** is the sum of (1) and (2).
Sediment oxygen consumption	**Total oxygen consumption** has three components: (1) seabed oxygen consumption, (2) water column oxygen consumption due to remineralization of resuspended POM, and (3) water column oxygen consumption due to remineralization of non-resuspended POM. **Sediment oxygen consumption** is the sum of (1) and (2).
Shelf region	The inner shelf and midshelf west of the Mississippi Delta and shallower than 50-m water depth (i.e., all of the shaded areas in Figure 1c).

entrainment of sediment, defined as both inorganic particles and particulate organic matter (POM), and pore water from the seabed into the water column can impact biogeochemical dynamics through a variety of processes. Observational and laboratory studies show that resuspension may alter rates of organic matter remineralization (e.g., Aller, 1998; Hartnett et al., 1998; Ståhlberg et al., 2006; Ziervogel et al., 2015), seabed-nutrient fluxes (e.g., Almroth et al., 2009; Fanning et al., 1982; Porter et al., 2010; Toussaint et al., 2014), and light attenuation (e.g., Cloern, 1987; Salisbury et al., 2004). In addition to local effects, resuspension and subsequent redistribution of material within coastal waters can alter the spatial and temporal distribution of POM, which may then affect biogeochemical dynamics (e.g., Abril et al., 1999; Christiansen et al., 1997; Goñi et al., 2007; Lampitt et al., 1995). However, observational and laboratory approaches for understanding and quantifying the role of seabed and near–bed processes on water column biogeochemistry are often limited by technological, safety, and/or cost constraints, and thus numerical models are important for interpolating and extrapolating results in space and time.

Previous modeling efforts have typically simplified seabed and near-bed processes, motivating the use of a relatively new process-based approach to analyze how resuspension affects bottom water biogeochemistry in coastal environments (Moriarty et al., 2017, and references therein). This paper expands on previous work utilizing the new approach to analyze the spatial variability of the role of resuspension on oxygen and ammonium dynamics. We specifically focused on the northern Gulf of Mexico, where the extent of summertime hypoxia is known to be sensitive to seabed and bottom boundary layer processes, as described below.
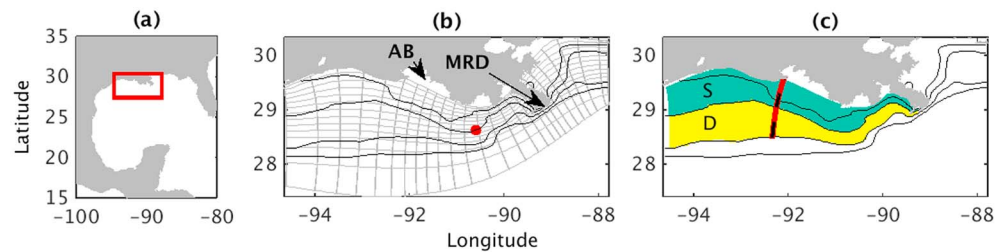
Figure 1. Study site maps showing (a) location within the Gulf of Mexico, (b) model grid, and (c) the *shallow* (S) and *deep* (D) regions of the inner shelf to midshelf considered in section 3. In (b), every box indicates 25 grid cells. Atchafalaya Bay and the Mississippi River Delta are denoted by *AB* and *MRD*, respectively. The red dot indicates the location of wind and wave data in Figure 2. In (c), the combined turquoise and yellow shading indicates the shelf region. The red and black line indicates the location of the transect in Figure 7. Black lines in (b) and (c) are bathymetric contours for 10, 20, 50, and 100 m.

1.1. The Role of Seabed and Near-Bed Processes in the Northern Gulf of Mexico

The northern Gulf of Mexico is a river-dominated shelf system characterized by a seasonally varying dynamic physical environment. The Mississippi River and its distributary, the Atchafalaya River (Figure 1), deliver freshwater, inorganic sediment, organic matter, and nutrients to the northern Gulf of Mexico shelf, where these terrestrial inputs are generally transported westward and offshore by shelf currents (e.g., Bianchi et al., 2010; Fry et al., 2015; Wright & Nittrouer, 1995; Wysocki et al., 2006; Zhang et al., 2012). Material deposited in shallow areas of the shelf (~0–20-m water depth) is subjected to high bed stresses and may be resuspended and redistributed across the shelf throughout the year, while hurricanes and storms can rework deposited sediments in both shallow and deeper regions (Allison et al., 2000; Corbett et al., 2004; Draut et al., 2005; Goñi et al., 2006; Kineke et al., 2006; Xu et al., 2011).

Summertime hypoxia develops on the shelf due to seasonally high temperatures and riverine delivery of nutrient inputs, as well as the presence of the river plume that facilitates stratification, limiting oxygen supply to bottom waters (e.g., Wiseman et al., 1997; Bianchi et al., 2010; Forrest et al., 2012; Yu, Fennel, Laurent, Murrell, & Lehrter, 2015). Unlike many regions where the location, extent, and fragmentation of hypoxia are constrained by bathymetry (e.g., Conley et al., 2009; Kemp et al., 2005), hypoxia in the northern Gulf of Mexico is typically observed near the Mississippi Delta where persistent stratification occurs, as well as in fragmented patches across the shelf that vary interannually in location and area, and possibly on shorter timescales as well (Rabalais et al., 2002). The hypoxic water on this shelf is a thin layer in the bottom water column, typically about 1–2 m thick (Fennel et al., 2016, and references therein), which indicates that it is particularly sensitive to seabed and bottom boundary layer processes.

Previously developed conceptual models for the formation and maintenance of hypoxia on the northern Gulf of Mexico shelf acknowledge that the processes affecting the formation of these low-oxygen areas vary spatially. Rowe and Chapman's (2002) conceptual diagram consists of three regions. Near the Mississippi Delta and along the coast, the high turbidity in their *Brown Water* limits phytoplankton growth and so hypoxia is fueled by remineralization of allochthonous POM. Further offshore and alongshore, high levels of primary production in their *Green Water* region, and remineralization of this autochthonous POM, cause hypoxia. Finally, the *Blue Water* region occurs even further offshore and alongshore where reduced nitrogen concentrations limit phytoplankton growth and hypoxia can occur due to advection of low-oxygen waters into the area and remineralization of organic matter. In the last decade, many studies have built on Rowe and Chapman's (2002) conceptual diagram by showing the importance of benthic processes, including remineralization, for oxygen consumption, especially in shallow areas and the western region of the hypoxic zone (e.g., Fennel et al., 2013, 2016; Feist et al., 2016; Hetland & DiMarco, 2008; Lehrter et al., 2012; McCarthy et al., 2013; Yu, Fennel, Laurent, Murrell, & Lehrter, 2015). Even weeks after POM deposition, nutrient fluxes from the seabed may further stimulate production, remineralization, and future oxygen demand, especially at the onset and end of hypoxic events (Eldridge & Morse, 2008).

Seabed and bottom boundary layer biogeochemical processes respond to cycles of erosion and deposition, although the effects have been less frequently studied than those due to factors such as temperature, redox conditions, and organic matter lability. Episodes of resuspension may entrain millimeters to centimeters of

previously deposited inorganic sediment and POM into the water column (e.g., Goñi et al., 2007; Xu et al., 2011). One study in the northern Gulf of Mexico found that these episodes of erosion could cause dissolved inorganic nitrogen concentrations to approximately double (Fanning et al., 1982).

Previous modeling efforts focused on the northern Gulf of Mexico have corroborated that oxygen and nitrogen dynamics are sensitive to seabed-water column fluxes, but the studies have simplified these processes (Feist et al., 2016; Fennel et al., 2013; Hetland & DiMarco, 2008; Laurent et al., 2016, 2017; Yu, Fennel, & Laurent, 2015; Yu, Fennel, Laurent, Murrell, & Lehrter, 2015). Fennel et al. (2013) found that using different parameterizations for seabed-water column fluxes of oxygen and nitrogen altered the estimated hypoxic area by over 100%. This sensitivity of the model results suggests that more realistic representation of the seabed and related processes in biogeochemical models may be important for understanding and predicting biogeochemical budgets, and the formation of hypoxic areas, in the northern Gulf of Mexico. Most biogeochemical models implemented for this region have neglected the role of resuspension. Exceptions include a one-dimensional model for carbon dynamics (Wainright & Hopkinson, 1997) and a three-dimensional study that accounted for the effect of resuspended sediment on light attenuation (Justić & Wang, 2014). However, to the best of our knowledge, no published study has focused on the effect of resuspension on remineralization, seabed-water column fluxes, and the distribution of POM on the northern Gulf of Mexico shelf or how changes in these processes affect oxygen and nitrogen dynamics.

1.2. Objectives

To address this gap, this study therefore used a numerical modeling approach that accounted for both sediment transport and biogeochemical processes to address how erosion and deposition may affect oxygen and ammonium dynamics in the northern Gulf of Mexico. Specifically, this study focused on how resuspension could alter bottom water biogeochemistry by changing remineralization of POM, seabed-water column fluxes, and oxidation of reduced chemical species that are entrained into the water column. For this analysis, we considered different timescales ranging from resuspension events to month-long periods that also included quiescent time periods, different areas of the shelf, and POM with varying remineralization rate constants and settling velocities.

2. Methods

To address the objectives listed above, a coupled hydrodynamic-sediment transport-biogeochemical model called HydroBioSed was implemented for the northern Gulf of Mexico. The following sections describe how the coupled model was modified from Moriarty et al. (2017; section 2.1) and implemented for the northern Gulf of Mexico (section 2.2), before describing the seven different model runs (section 2.3) and analysis (section 2.4).

2.1. Standard Model Description

Model formulations for HydroBioSed were previously described in detail in Moriarty et al. (2017) but are also summarized in this paragraph. Modeled processes in HydroBioSed account for advection of water, biogeochemical tracers, and inorganic particles; sinking and deposition of POM to the seabed; subsequent resuspension or storage of POM in the seabed; remineralization of POM and oxidation of reduced chemical species in both the water column and seabed; diffusion of dissolved chemical species across the seabed-water interface; and biodiffusion of particles and solutes within the seabed. We used the version of HydroBioSed without POM repartitioning (see Figures 1a and 1c in Moriarty et al., 2017). This coupled model (Moriarty et al., 2017) builds on the Regional Ocean Modeling System (ROMS) framework (Haidvogel et al., 2000, 2008; Shchepetkin, 2003; Shchepetkin & McWilliams, 2009), the Community Sediment Transport Modeling System (CSTMS; Warner et al., 2008), the Fennel et al. (2006, 2008, 2011) water column biogeochemistry model, and the Soetaert et al. (1996a, 1996b) seabed diagenesis model. HydroBioSed was previously implemented for the Rhône shelf as a quasi-one-dimensional model on a 5 by 6 cell grid with spatially uniform forcing and periodic boundary conditions (see definitions in Table 1).

To represent the northern Gulf of Mexico, the formulations described in Moriarty et al. (2017) were adapted for use in a spatially varying three-dimensional model and for a site having different environmental conditions. Specific modifications include open boundary conditions appropriate for the three-dimensional model and slight alterations to the seabed layering scheme to account for a wider range of erosional and

depositional conditions. Additionally, the version of the model used in Moriarty et al. (2017) used a technique called nudging (see definition in Table 1) to keep water column nutrient and oxygen concentrations near observed values. For the northern Gulf of Mexico, however, the model implementation allowed all state variables to evolve freely as prescribed by the water column biogeochemical model of Fennel et al. (2006, 2008, 2011). Moriarty et al. (2017) also assumed that a certain fraction of deposited organic matter was labile versus semilabile (note that semilabile material was called refractory in the earlier manuscript) because it was a one-dimensional model implementation. In contrast, for the current Gulf of Mexico implementation all POM produced on the shelf was assumed to be labile, whereas the rivers delivered both labile and semilabile POM. Thus, the ratio of labile versus semilabile POM that was deposited on the seabed varied depending on primary production, riverine inputs, and circulation. Finally, rates of remineralization and biodiffusion (i.e., vertical mixing within the seabed, including bioturbation as described in Sherwood et al., 2018) were parameterized to vary with temperature, as described in Laurent et al. (2016), who optimized a steady state one-dimensional version of the Soetaert et al. (1996a, 1996b) model for two sites on the northern Gulf of Mexico shelf.

2.1.1. Parameterization of POM

HydroBioSed's parameterizations of POM were presented in Moriarty et al. (2017) and the above section, but additional details are provided here because they are critical for understanding this study's results. In the model, POM in the water column is divided into distinct classes, including phytoplankton, zooplankton, small detritus, large detritus, labile aggregates, and semilabile aggregates. Each POM class was assigned properties, such as a characteristic settling velocity, remineralization rate constant, and critical stress for erosion (see Table 2). Note that these properties do not vary in time or space, except when material is transferred between the seabed and water column. The *net* remineralization rate constants, settling velocities, and critical stresses for erosion in a specific grid cell, or for a given pool of POM, may vary, however, depending on the proportion of POM that is plankton, detritus, or aggregates.

When POM settles on the seabed, phytoplankton, small detritus, large detritus, and labile aggregates become incorporated into the labile seabed organic matter class, whereas semilabile aggregates become semilabile seabed organic matter. The fraction of labile versus semilabile POM in the seabed therefore depends on the depositional history of organic matter in that location; unlike some seabed diagenetic models (e.g., Soetaert et al., 1996a, 1996b; the one-dimensional models within Laurent et al., 2016), HydroBioSed does not assume that a certain fraction of the depositing organic matter is labile or semilabile when implemented in three dimensions. Upon deposition, POM is initially incorporated into the surficial seabed layer, but this material may be incorporated into deeper layers or become resuspended based on the seabed layering routines described in Warner et al. (2008) and Moriarty et al. (2017). Note that these routines cause recently deposited POM and inorganic sediment to generally be resuspended before material that is deeper in the seabed, although bioturbation may vertically mix some material among different seabed layers. Also, note that POM in deeper layers can be resuspended if it is reincorporated into the surficial seabed layer during time periods of extensive erosion. Consistent with Warner et al. (2008) and Moriarty et al. (2017), material from a seabed POM class may be resuspended when the modeled bed shear stress exceeds the material's critical stress for erosion. Upon resuspension, labile seabed organic matter is incorporated into the labile aggregates variable, whereas semilabile seabed organic matter becomes semilabile aggregates because we used the version of HydroBioSed without repartitioning of POM (see Moriarty et al., 2017).

Finally, in addition to the transport processes described above, POM concentrations in the model change depending on primary production, remineralization, and other biogeochemical processes, as well as riverine delivery (see Fennel et al., 2006; Soetaert et al., 1996a). Consistent with Fennel et al. (2013), POM remineralization in the water column is limited by low oxygen but does not include denitrification or anaerobic remineralization because anoxic conditions rarely occur in the water column in our study region. Seabed routines do account for denitrification and anaerobic remineralization, but remineralization does not vary with oxygen levels, based on Soetaert et al. (1996a). Choice of remineralization rate constants and other model inputs and parameters for the northern Gulf of Mexico model implementation are detailed below.

2.2. Standard Model Implementation

The model grid and hydrodynamic forcing for the coupled northern Gulf of Mexico model implementation were based on Hetland and DiMarco (2012) but also accounted for wave-induced bed stress. The model

Table 2
Parameters for the Standard Model Implementation for the Northern Gulf of Mexico Shelf

Parameter		Modeled value	Source for observed/ literature values
Sediment Transport Parameters (Selected)			
Partitioning of sediment into classes	MI River	Small flocs: 50% Large flocs: 50%	Xu et al. (2011); Williams et al. (2006)
	Atchafalaya River	Small flocs: 90% Large flocs: 10%	
	Seabed	Large flocs: spatially variable Sand: spatially variable	
Settling velocity	MI River	Small flocs: 0.1 mm/s Large flocs: 1.0 mm/s	Xu et al. (2016)
	Atchafalaya River	Small flocs: 0.1 mm/s Large flocs: 1.0 mm/s	
	Seabed	Large flocs: 0.1 mm/s Sand: 1.0 mm/s	
Critical bed shear stress for erosion	MI River	Small flocs: 0.11 Pa Large flocs: 0.11 Pa	Xu et al. (2011)
	Atchafalaya River	Small flocs: 0.03 Pa Large flocs: 0.03 Pa	
	Seabed	Large flocs: 0.11 Pa Sand: 0.13 Pa	
Erosion rate parameter		3×10^{-4} kg $\cdot$ m^2 $\cdot$ s	Xu et al. (2016)
Porosity		0.8	Xu et al. (2011); Laurent et al. (2016)
Sediment density		2,650 kg/m^3	Xu et al. (2011)
Biogeochemical Parameters			
Water Column Rates (Selected)			
Light attenuation due to:		Seawater: 0.04 m^{-1}	Fennel et al. (2006, 2013)
		Chlorophyll: 0.02486 (mg Chl m^2)$^{-1}$	Fennel et al. (2006, 2013)
Maximum nitrification rate constant		0.05 d^{-1}	Fennel et al. (2006, 2013)
Phytoplankton and zooplankton carbon: nitrogen molar ratio		6.625 mol C (mol N)$^{-1}$	Fennel et al. (2006, 2013)
Coagulation rate of small detritus and phytoplankton		0.005 (mmol N m^{-3})$^{-1}$ d^{-1}	Fennel et al. (2006, 2013)
Organic matter remineralization rates		Small detritus: 0.3 d^{-1} Large detritus: 0.1 d^{-1} Labile aggregates: 0.1 d^{-1} Semilabile aggregates: 0.1 d^{-1}	Yu, Fennel, Laurent, Murrell, and Lehrter (2015), Devereux et al. (2015), Wainright and Hopkinson (1997), and references therein
Settling (sinking) velocity		Phytoplankton: 0.1 m d^{-1} Small detritus: 0.1 m d^{-1} Large detritus: 1.0 m d^{-1} Aggregates: 8.64 m d^{-1}	Fennel et al. (2006; 2013) and Wakeham et al. (2009)
POM critical bed shear stress		0.11 Pa	Assumed to be equal to seabed flocs
POM erosion rate parameter		3×10^{-4} kg $\cdot$ m^2 $\cdot$ s	Assumed to be equal to seabed flocs
Partitioning of POM in river input		Small detritus: 16% Semilabile aggregates: 84%	Fry et al. (2015)
Seabed Rates (Selected)			
Remineralization rate constants of seabed organic matter		Labile organic matter: 0.1 d^{-1} Semilabile Organic Matter: 5.8×10^{-5} d^{-1}	Laurent et al. (2016)
Coefficients for Q_{10} temperature-remineralization relationship		Base temperature: 30 °C Q_{10} parameter: 3	Laurent et al. (2016)
Nitrogen to carbon molar ratio for seabed organic matter		Labile Organic Matter: 0.15 Semilabile Organic Matter: 0.1	Laurent et al. (2016)
Maximum nitrification rate		100 d^{-1}	Laurent et al. (2016) and Devereux et al. (2015)
Maximum oxidation rate of oxygen demand units		11.45 d^{-1}	Laurent et al. (2016)
Base biodiffusion coefficients for sediment and POM		Maximum: 2.785×10^{-11} m^2/s Minimum: 0 m^2/s	Laurent et al. (2016)
Base biodiffusion coefficients for dissolved solutes		O_2: 11.05×10^{-10} m^2/s	Laurent et al. (2016)

Table 2 *(continued)*

Parameter	Modeled value	Source for observed/ literature values
	NO_3: 9.78×10^{-10} m^2/s	
	NH_4: 9.803×10^{-10} m^2/s^{-1}	
	ODU: 9.7451×10^{-10} m^2/s	
Base temperature for Q_{10} temperature-biodiffusion relationship (for particulates)	20 °C	Laurent et al. (2016)
Q_{10} parameter for temperature-biodiffusion relationship (for particulates)	2	Laurent et al. (2016)
Coefficients for temperature-biodiffusion relationship (for solutes)	O_2: 4.468×10^{-11} m^2/s	Laurent et al. (2016)
	NO_3: 3.507×10^{-11} m^2/s	
	NH_4: 3.889×10^{-11} m^2/s	
	ODU: 2.801×10^{-11} m^2/s	
Depth in seabed for which maximum biodiffusion coefficient is used	0–1-cm deep	Laurent et al. (2016)
Depth in seabed for which minimum biodiffusion coefficient is used	Over 3-cm deep	Laurent et al. (2016)
Depth in seabed for which the biodiffusion coefficient is linearly interpolated from maximum to minimum value	1–3-cm deep	Laurent et al. (2016)

Note. Mississippi is abbreviated as MI.

grid specifically focused on the area west of the Mississippi River delta where seasonal hypoxia develops, and it has been previously used for multiple modeling studies of sediment transport and hypoxia (e.g., Fennel et al., 2013, 2016; Laurent et al., 2016, 2017; Xu et al., 2011, 2016; Yu, Fennel, & Laurent, 2015; Yu, Fennel, Laurent, Murrell, & Lehrter, 2015). Lateral open boundary conditions were consistent with Hetland and DiMarco (2012) and were based on Chapman (1985) for sea surface height, Flather (1976) for depth-averaged momentum, and Marchesiello et al.'s (2001) radiation conditions for depth-varying momentum and tracers. Tracers were also nudged to monthly climatological data from Boyer et al. (2006) and the National Oceanographic Data Center at the open boundaries, as described in Yu, Fennel, Laurent, Murrell, and Lehrter (2015). Model forcing also included atmospheric data with winds provided every 3 hr from da Silva et al. (1994a, 1994b; as described in Fennel et al., 2013), daily river discharge as estimated by the Army Corps of Engineers (as described in Yu, Fennel, Laurent, Murrell, & Lehrter, 2015), and the shortwave radiation parameterization from Fennel et al. (2016). The U.S. National Oceanic and Atmospheric Administration (NOAA)'s Wave Watch III (WW3; Tolman et al., 2002) model estimates of significant wave height, dominant surface wave period, and dominant wave direction were used to estimate representative bottom wave period and representative bottom orbital velocity every 6 hr, following methods from Wiberg and Sherwood (2008). Bed stress was calculated using the bottom boundary layer parameterization based on Madsen (1994), as described in Warner et al. (2008), consistent with previous Gulf of Mexico sediment transport model implementations (Xu et al., 2011, 2016). Table 2 provides additional parameters.

Inputs and parameters for the sediment transport, water column biogeochemistry, and seabed biogeochemistry modules were configured based on Xu et al. (2011, 2016), Fennel et al. (2013), and Laurent et al. (2016), respectively, and are detailed in Table 2. For implementation over multiple years and the entire model grid, two rate constants from the seabed biogeochemical module were adjusted to better match observations of seabed-water column fluxes (Tables 2 and 3). Specifically, the nitrification rate constant from Laurent et al. (2016) was doubled from 50 to 100 d^{-1}, and the labile POM remineralization rate constant was increased from 0.01 to 0.1 d^{-1}. This model implementation also differed from Xu et al. (2011, 2016) by allowing sediment concentrations to affect the density equation of state (see Warner et al., 2008). Sediment classes were distinguished by source (i.e., seabed, Mississippi River, or Atchafalaya River). POM classes were characterized by types of plankton and detritus based on Fennel et al. (2006, 2013; i.e., phytoplankton, zooplankton, and small and large detritus) and by lability (labile and semilabile aggregates). River inputs were provided by the U.S. Geological Survey for inorganic sediment (Xu et al., 2011, 2016) and biogeochemical tracers (Aulenbach et al., 2007, as described in Fennel et al., 2013). In contrast to Fennel et al.'s (2013) assumption that all POM delivered by the Mississippi and Atchafalaya Rivers was small detritus, we assumed that 84% of this material was semilabile

Table 3
Comparison Between Estimates From the Standard Model Versus Observations of Bottom Water and Seabed Properties and Fluxes

	Standard model run		Observation	
	Mean ± Standard Deviation	Range	Range	Citation
Bottom water POC (mmol C m^{-3})	34 ± 110	0–7,800	0–225	Fry et al. (2015)
			0–417	Goñi et al. (2006)
Seabed-water column O$_2$ Flux (mmol O$_2$ m^{-2} d^{-1})	−4.7 ± 4.1	−46–2.0	~ −25–0	Lehrter et al. (2012)
			−14.05–0	Devereux et al. (2015)
			−56.4– −0.82	Rowe et al. (2002)
			−43.3– −9.94	McCarthy et al. (2013)
			−23.3– −1.3	Murrell and Lehrter (2011)
Seabed-water column NH$_4$ Flux (mmol N m^{-2} d^{-1})	−0.93 ± 0.81	−11–2.1	−0.17–3.84	Lehrter et al. (2012)
			0.8–4.4	Rowe et al. (2002)
			−0.11–4.92	McCarthy et al. (2015)
Bottom water O$_2$ respiration (mmol O$_2$ m^{-3} d^{-1})	4.3 ± 14	0.0–1,700	3.84–106	McCarthy et al. (2013)
			1.4–14.0	Murrell and Lehrter (2011)
			~0–46.6	Murrell et al. (2013)

Note. Positive fluxes indicate fluxes directed out of the seabed. Model estimates are from June 2006; time period of observations are given in each publication.

aggregates based on Fry et al. (2015). POM remineralization rate constants were chosen based on literature values (Devereux et al., 2015; Laurent et al., 2016), as well as to match observations of POM, oxygen, and ammonium concentrations, and seabed-water column fluxes on the northern Gulf of Mexico shelf (Table 3, and references therein). POM settling velocities were based on Fennel et al. (2013) for plankton and detrital classes; organic aggregates were assumed to have the same settling velocity as the inorganic small flocs from Xu et al. (2011, 2016); this settling velocity was consistent with grain size observations from Wakeham et al. (2009). Similarly, due to lack of observational data, a single value of critical shear stress for erosion was used for all seabed POM and fine-grained inorganic sediments and was chosen based on Xu et al. (2011, 2016).

Although remineralization rate constants for each class of POM were constant in time and space except when material was transferred between the seabed and water column, the combination of parameters accounted for many known organic matter processes. First, the remineralization rate constant for labile aggregates and seabed organic matter was assumed to be the same in the water column and seabed. In contrast, the remineralization rate constant was assumed to be faster for semilabile aggregates compared to semilabile seabed organic matter because of the higher oxygen concentrations in the water column. This assumption is consistent with theories that oxygen affects the remineralization of semilabile and refractory organic matter remineralization more than labile material (Andersen, 1996; Dauwe et al., 2001) and also that resuspension increases remineralization (Ståhlberg et al., 2006), likely due to increased oxygen exposure and other factors (e.g., Aller, 1994; Arzayus & Canuel, 2004; Caradec et al., 2004; Gilbert et al., 2016; Sun et al., 2002; Wakeham & Canuel, 2006). The slower rate constant for semilabile seabed organic matter also allowed the net remineralization rate constant in the seabed to change in time and depth. For example, for a given pool of seabed POM, the net remineralization rate constant decreased in time as the labile POM was decomposed until only semilabile material remained. Similarly, because it takes time for a given pool of POM to become buried, net remineralization rate constants also decreased with depth into the seabed until no labile organic matter remained. Note that the difference in labile versus semilabile remineralization rate constants also implies that surficial seabed layers had a larger fraction of labile organic matter compared to deeper layers, and so resuspended organic matter was relatively rich in labile organic matter. This effect occurred despite the use of a critical erosion stress that was the same for both organic and inorganic sediment and was the same for both labile and semilabile POM. Once resuspended, we note that all organic matter except for small detritus was given the same remineralization rate constant; despite this assumption, however, the remineralization of a pool of suspended POM decreased in time as decomposition of some of the organic matter decreased POM availability. Overall, these rates were chosen to represent observations of oxygen concentrations, seabed-water column fluxes, and hypoxia on the northern Gulf of Mexico shelf and were consistent with previously used values for the northern Gulf of Mexico (see Table 2).
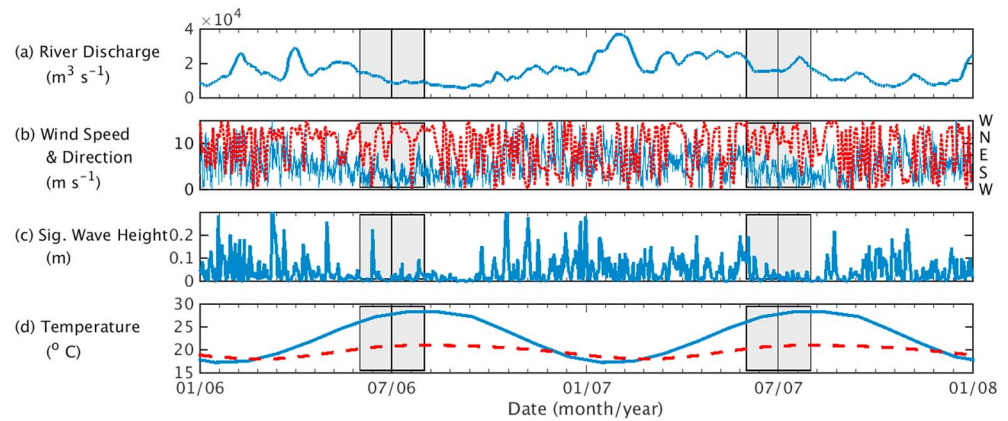
Figure 2. Time series of model forcing, including (a) the combined water discharge of the Mississippi and Atchafalaya Rivers, (b) wind speed (blue line; left axis) and direction (red dots; right axis) toward which winds are blowing, (c) significant wave height, and (d) climatological air temperature (blue solid line) and depth-averaged temperature at the open boundary (red dashed line). Wind and wave data were provided for a location on the midshelf at 20-m water depth (location shown in Figure 1). Shading indicates the time periods on which this paper focuses, including June and July 2006 and 2007. Data sources and temporal resolution are provided in section 2.2.

2.3. Model Runs

The coupled model described above was run for 2006–2007, which were both relatively typical years for river discharge, wave energy, and winds. Compared to 2007, 2006 had lower discharge, more easterly winds, and higher wave energy based on data from NDBC buoys 42040 and 42007 and the Army Corps of Engineers (Figure 2 and Table 2). Although these years may not completely represent the full range of interannual variability of the northern Gulf of Mexico, they are adequate for looking at the impact of short-term events over month-long timescales. Initial model fields were obtained by repeating the 2006–2007 model run twice, until temporal variations between spatially averaged data were minimal, and then the final time step of the spin-up simulation was used as the initial condition for the *standard model run*. Model output was saved every 12 hr.

In addition to the standard model run, sensitivity tests were used to estimate how various parameter choices affected modeled biogeochemical dynamics. Sensitivity tests were identical to the standard model run, except as noted in Table 4, and focused on resuspension, remineralization rate constants, and organic matter settling velocities to explore the effect of resuspended POM on bottom water biogeochemistry. For example, the no-resuspension model run was identical to the standard model run, except that the erosion rate parameter was set to zero. Additional sensitivity tests varied POM remineralization rate constants and settling velocities by factors of 5. Although estimates for both parameters in the literature vary over multiple orders of magnitude (e.g., 0.001–32 d^{-1} for remineralization rate constant and 0.1–28 m/d for settling velocity;

Table 4
Model Run Characteristics

Name of model run (abbreviation)	Change compared to the standard model run	Temporal coverage of model run(s)
Standard (ST)	N/A	1 January 2006 to 31 December 2007
No-resuspension (NR)	Identical to standard model run, except that resuspension was prevented from occurring by changing the erosion rate parameter to zero for both inorganic and organic sediment	1–30 June 2006, 1–31 July 2006, 1–30 June, 2007, and 1–31 July 2007
Fast settling (FS)	Identical to standard model run, except that settling velocities of inorganic sediment, organic aggregates, and large detritus were increased by a factor of 5	1–30 June 2006
Slow settling(SS)	Identical to standard model run, except that settling velocities of inorganic sediment, organic aggregates, and large detritus were decreased by a factor of 5	1–30 June 2006
Fast remineralization (FR)	Identical to standard model run, except that remineralization rate constants of large detritus, organic aggregates and labile seabed organic matter were increased by a factor of 5	1–30 June 2006
Slow remineralization (SR)	Identical to standard model run, except that remineralization rate constants of large detritus, organic aggregates and labile seabed organic matter were decreased by a factor of 5	1–30 June 2006

Fennel et al., 2006; Patten et al., 1966; Testa et al., 2013; Wainright & Hopkinson, 1997; Yu, Fennel, Laurent, Murrell, & Lehrter, 2015), we chose to vary parameters by factors of 5 because larger variations in the parameters produced results similar to the no-resuspension model run (for fast-settling and slow-remineralization sensitivity tests) or produced unreasonable model estimates (i.e., the entire shelf became hypoxic in slow-settling and fast-remineralization sensitivity tests). Sensitivity tests were initialized with modeled fields from the standard model run from 1 June 2006, 1 July 2006, 1 June 2007, or 1 July 2007, and each simulation was run for 1 month (see Table 4). Model analysis focused on these time periods because Gulf of Mexico hypoxia is typically observed in July (e.g., Rabalais et al., 2002). In both 2006 and 2007, June had similar environmental conditions to July but included larger wave-induced resuspension events (Figure 2c).

2.4. Model Analysis

Model analysis focused on how seabed resuspension affected biogeochemical processes within the bottom water column and their effect on oxygen and ammonium dynamics. Seabed-water column fluxes of oxygen and ammonium, and oxidation of ammonium and other reduced chemical species, were included in the model; however, these were not especially sensitive to resuspension. In contrast, POM remineralization was characterized by large, episodic changes during resuspension events, and so sections 3 and 4 primarily focus on this process. The standard model run was evaluated by comparing it to observations from the northern Gulf of Mexico of particulate organic carbon (POC) concentrations, effective water column (i.e., oxygen consumption) and seabed fluxes of O_2 and NH_4.

Analysis focused primarily on a wave event in June 2006 and the relatively quiescent month of July 2006, but time-averaged estimates for month-long periods during summer 2007 are also discussed. To estimate the effect of resuspension on the biogeochemical processes listed above, we analyzed results from the standard model run and the sensitivity tests. Specifically, estimates from the standard model run during cycles of erosion and deposition were compared to those from quiescent time periods. The role of resuspension was further quantified by comparing results from the standard model run to those from the no-resuspension sensitivity tests. Finally, calculations from the sensitivity tests were compared to those from the standard model run to examine the sensitivity of the results to parameters affecting remineralization and the residence time of particles in the water column.

For this analysis, the following definitions were used. *Bottom water* concentrations and rates indicated estimates for locations 1 m above the seabed in the model. In locations where the bottom grid cell thickness exceeded 1 m, results were linearly extrapolated to locations 1 m above the seabed. Except when the text explicitly states otherwise, model estimates were averaged over the *shelf region*, which was defined as the inner shelf and midshelf (shallower than 50-m water depth) region of the model grid west of the Mississippi Delta. The shaded regions in Figure 1c identify the shelf region, which had a spatial extent of 54×10^3 km^2. The *remineralization rate constant* is a temporally and spatially constant model parameter that is provided for each class of POM with units of inverse time. In contrast, the text will use the terms *effective remineralization rate* and *remineralization* to refer to the temporal rate of change in POC concentrations due to decomposition, with a unit of carbon concentration * $time^{-1}$. Note that the molar ratio of carbon to dissolved oxygen ($C:O_2$) was assumed to equal 1.

Finally, *sediment oxygen consumption* was defined as the sum of (1) seabed oxygen consumption, defined as the net flux of oxygen into the seabed, and (2) oxygen consumption related to resuspended POM, that is, due to remineralization and oxidation of the reduced chemical species (see Table 1). Note that as we define it, sediment oxygen consumption is one component of the total oxygen consumption because sediment oxygen consumption does not account for changes in oxygen related to remineralization of organic matter that has never been deposited. Similarly, *sediment ammonium production* was defined as the sum of (1) the net flux of ammonium out of the seabed and (2) changes in ammonium production due to remineralization of resuspended POM; note that sediment ammonium production could be negative if the net flux of ammonium was directed into the seabed (see Table 1). Sediment ammonium production differed from total ammonium production because it did not account for changes in ammonium related to remineralization of organic matter that had never been deposited. Note that definitions of sediment oxygen consumption vary in the scientific literature, typically depending on the experimental design, and may or may not include bottom water column oxygen consumption in addition to seabed oxygen consumption (Sloth et al., 1996; Berg & Huettel, 2008; Toussaint et al., 2014). We chose our definition because it includes all sources of oxygen

consumption that are often assumed to be included in numerical models' estimates of sediment oxygen consumption (e.g., Feist et al., 2016; Fennel et al., 2013; Moriarty et al., 2017).

Estimates of sediment oxygen consumption and ammonium production were calculated from model results as described below. For the no-resuspension sensitivity test, resuspension-induced oxygen consumption and ammonium production were zero, so the sediment oxygen consumption equaled the seabed oxygen consumption; sediment ammonium production was equivalent to the net flux of ammonium out of the seabed. For the standard model run, in contrast, sediment oxygen consumption equaled the sum of the seabed oxygen consumption, as well as the resuspension-induced oxygen consumption; the latter term equaled the water column oxygen consumption from the standard model run minus oxygen consumption from the no-resuspension sensitivity test. Likewise, sediment ammonium production in the standard model run equaled the net flux of ammonium out of the seabed, as well as the resuspension-induced ammonium production; the latter term equaled the water column ammonium production from the standard model run minus ammonium production from the no-resuspension sensitivity test. In all cases, rates were depth integrated over the entire water column to capture the effect of POM entrained from the seabed to the top of the water column.

3. Results

Resuspension caused large, episodic changes in POM remineralization, which generally decreased oxygen concentrations and increased ammonium concentrations in the bottom water column in the model. This section first evaluates the model results by comparing them to observations (section 3.1), focusing on POC concentrations, oxygen consumption, and seabed-water column fluxes. The following sections focus on the effect of resuspension on bottom water biogeochemistry during individual events (section 3.2) and over month-long timescales (section 3.3), with an emphasis on the spatial variability.

3.1. Comparison of Standard Model Results to Observations

Overall, model estimates representing summer 2006 captured the patterns of POC concentrations observed in 2006–2010 by Fry et al. (2015). Although peaks in modeled bottom water POC concentrations generally occurred in shallower water compared to observations, both data sets indicated that maximum values decreased from ~200 mmol C m^{-3} in shallow waters of 10–25-m water depth, to ~50 mmol C m^{-3} in regions deeper than 35 m (Figures 3a and 3b). Additionally, in surface waters, modeled POC concentrations peaked in saltier water compared to observations, but both data sets estimated that POC concentrations peaked in waters with salinity of 5–30 PSU, and were lower in salinities of 0–5 PSU and above 30 PSU (Figures 3c and 3d).

The coupled model also reproduced observed patterns of seabed-water column fluxes and respiration. For example, modeled rates of respiration and seabed fluxes (Table 3) indicated that water column processes were a larger oxygen sink below the pycnocline than seabed processes, consistent with observations from McCarthy et al. (2013). Specifically, the model estimated that the mean seabed oxygen flux accounted for 6–35% of the mean oxygen consumption below the pycnocline, similar to McCarthy et al.'s (2013) estimated range of 1–53%. Note that the above estimates were calculated using values from Table 3, and using McCarthy et al.'s (2013) assumption that localized, or *point*, estimates of respiration in the bottom water column could be applied to the entire region below the pycnocline, located from zero to 2–15 m above the seabed. The upper range of McCarthy et al.'s (2013) estimate, 53%, likely exceeded the upper range of modeled estimates, 35%, because the former values were based on shipboard experiments that simulated fair-weather, not resuspension, conditions. Resuspension typically increases water column oxygen consumption while maintaining or decreasing seabed oxygen consumption (e.g., Moriarty et al., 2017), at least partially explaining the difference between the modeled and observed estimates. Additionally, the model's neglect of some nitrogen cycle processes, for example, anaerobic oxidation of ammonium (anammox) and dissimilatory nitrate reduction to ammonium, likely caused HydroBioSed to more poorly represent seabed-water column fluxes of ammonium, compared to seabed-water column fluxes of oxygen.

Model estimates of POC concentration, respiration, and seabed fluxes generally had larger ranges than those derived from field data (Table 3), which is not surprising because, compared to observational studies, the model run covered a longer time period, a wider range of spatial locations, and a broader range of environmental conditions, including both storms and quiescent periods. For example, in some instances, the model
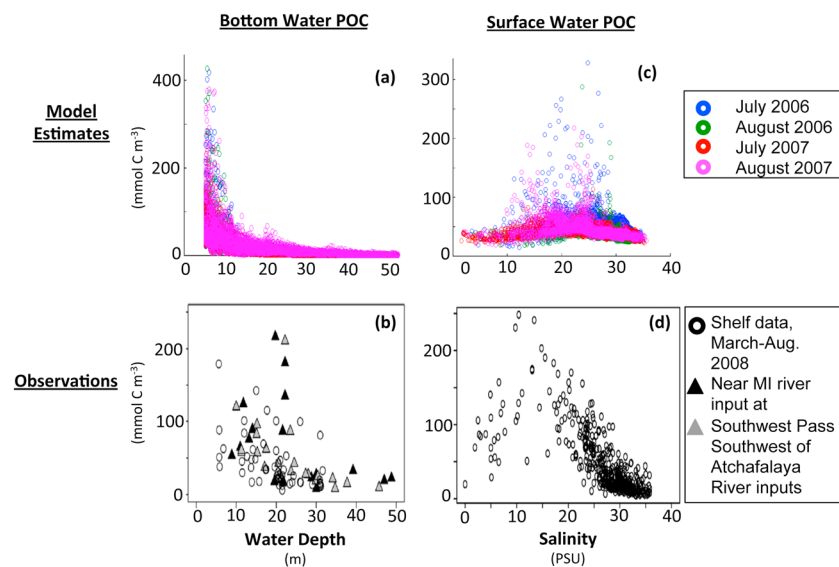
Figure 3. POC concentrations. (a) Monthly averaged model estimates of POC 1 m above the bed for each grid cell in the shelf region, for July 2006, August 2006, July 2007, and August 2007. (b) From Fry et al. (2015); observed POC from approximately the bottom 2 m of the water column for two offshore transects near the MI River delta and westward of Atchafalaya River. Shading and shape indicate different times and locations of collection (see legend and Fry et al., 2015); values are predominantly from summer 2008 but include some estimates from other months in 2008. (c) Monthly averaged model estimates of POC in the top grid cell of the model for each grid cell in the shelf region, for July 2006, August 2006, July 2007, and August 2007. (d) From Fry et al. (2015); observed surface water POC for 2006–2010.

estimated that oxygen fluxes were directed out of the seabed (Table 3) during the beginning of erosional periods when layers of oxic pore water from surficial sediments were entrained into the water column. However, these ephemeral events are difficult to observe during conventional field studies. Similarly, model estimates of respiration in the bottom grid cells at times exceeded the maximum observed values (Table 3). This is not surprising, because modeled POC concentrations in these grid cells also exceeded observed values (Table 3), which can be at least partially attributed to the relatively sparse temporal and spatial sampling schemes achievable by observational techniques compared to the higher-resolution model. Despite some differences with various observational data sets, the model estimates captured many expected patterns of shelf biogeochemistry, including POC peaks near the surface and bottom of the water column, and seasonal near-bed hypoxia driven by both water column and seabed oxygen consumption. The remainder of section 3 focuses on analysis of these model results.

3.2. Effect of Resuspension Over Event Timescales

Summer conditions in 2006 and 2007 were generally characterized by low-energy hydrodynamic conditions (Figure 2), but energetic waves did cause widespread resuspension to occur during 10–23 June 2006, 24–31 July 2006, 1–11 June 2007, 16–23 June 2007, and 27 July 2007. The response of bottom water column biogeochemistry to erosion and deposition was similar during these five periods, so the remainder of this section focuses on model estimates from the 13-day event, 10–23 June 2006, hereafter referred to as the *June 2006 event*. During the June 2006 event, bed shear stresses exceeded 2 Pa in regions as deep as 40 m and exceeded the 0.13-Pa threshold for resuspension in water depths up to about 90 m (Figure 4). This event is contrasted with a 23-day period with low-energy hydrodynamic conditions from 1–23 July 2006 (Figure 2) when bed stresses were only sufficiently high to resuspend sediment a few times.

During the June 2006 event, the standard model run estimated that seabed organic matter was entrained into the water column when bed stresses were high, increasing estimated concentrations of POC from 1–20 to 60–320 mmol C m^{-3} (Figures 5a and 5b). This additional source of POC resulted in the median effective remineralization rate increasing from <1 to 15 mmol C m^{-3} d^{-1} during this June 2006 event (Figure 5e). In contrast to June, POC concentrations in 1–23 July 2006 remained low, but median values did increase from about 1 to 40 mmol C m^{-3} during some of the smaller resuspension events during this time period
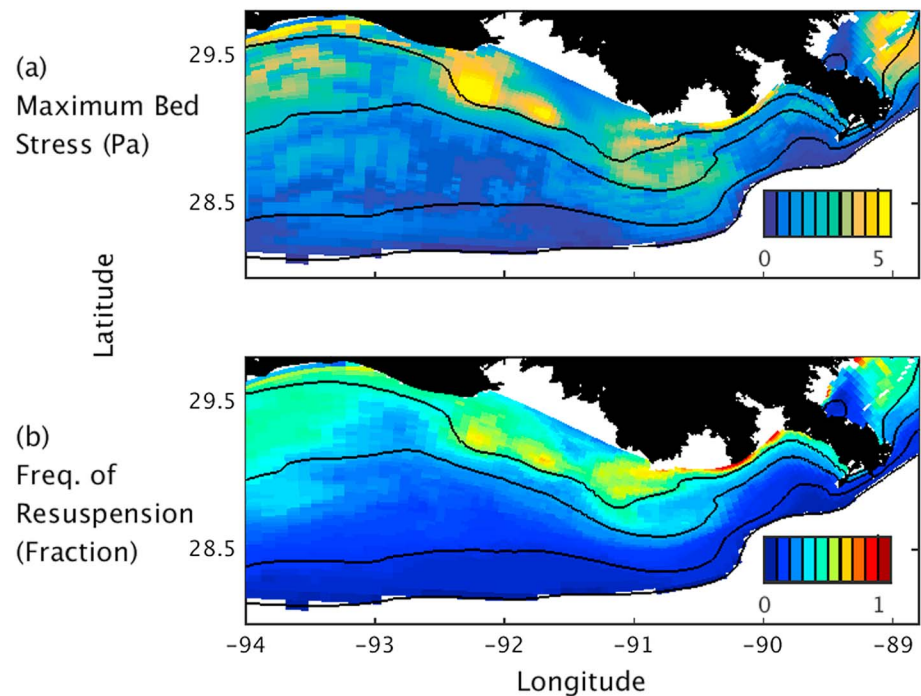
Figure 4. Model-estimated (a) maximum value of time-averaged wave- and current-induced bed stress during the June 2006 event and (b) frequency of resuspension for June 2006. Frequency of resuspension was calculated as the proportion of time when bed stress exceeded 0.1 Pa. Bathymetric contours (black lines) indicate water depths of 10, 20, 50, and 100 m.

(Figures 6a and 6b). Consistent with the June resuspension event, effective remineralization rates during these smaller events increased from medians of 0.1 to 6 mmol C m^{-3} d^{-1} (Figure 6e).

Resuspension also increased nitrification and seabed-water column fluxes of ammonium and oxygen, but the changes in median values were small in the standard model run. During the June event, resuspension increased median bottom water nitrification rates from 0.03 to 0.04 mmol N m^{-3} d^{-1}. The median flux of oxygen into the seabed also changed from 7 to 8 mmol O$_2$ m^{-2} d^{-1} during the June event. Finally, the median value of seabed-water column fluxes of ammonium remained at about 1 mmol O$_2$ m^{-2} d^{-1} out of the seabed during both quiescent periods and the resuspension event. Overall, these resuspension-induced changes in bottom water nitrification and seabed fluxes were small compared to changes in remineralization, so the remainder of the paper focuses on the latter process, as well as changes in oxygen and ammonium concentrations.

Consistent with the changes in processes described above, sediment oxygen consumption and sediment ammonium production peaked during resuspension events in the standard model run (Figures 5f, 5g, 6f, and 6g). During the June 2006 event, median values of sediment oxygen consumption increased from about 7 to 50 mmol O$_2$ m^{-2} d^{-1} (Figures 5f). Median sediment oxygen consumption also increased to about 20 mmol O$_2$ m^{-2} d^{-1} during the smaller episodes of resuspension in 1–23 July 2006 (Figures 6f). Similarly, median sediment ammonium production increased from about −1 mmol N m^{-2} d^{-1}, due to ammonium fluxes directed into the seabed, to 6 mmol N m^{-2} d^{-1}, due to remineralization of organic matter during resuspension events in June 2006 (Figure 5g). During the smaller resuspension events in July, sediment ammonium production increased to 1 mmol N m^{-2} d^{-1} (Figure 6g).

Supplementing the time series analysis of results from the standard model run, a comparison of estimates between the standard and no-resuspension simulations further indicated that entrainment of POC into the water column increased remineralization, sediment oxygen consumption, and sediment ammonium production. For example, median estimates of bottom water remineralization in the standard model run exceeded that in the no-resuspension simulation by ~14 mmol O$_2$ m^{-3} d^{-1} during the June 2006 event and by 6 mmol
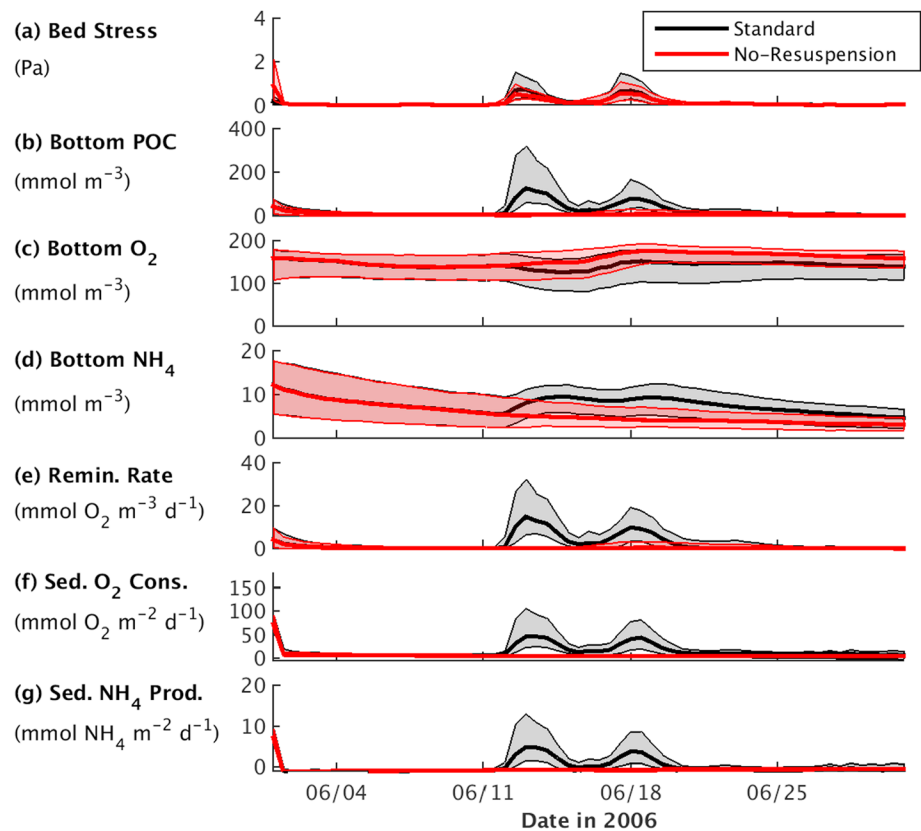
Figure 5. Time series of (a) bed stress, bottom water concentrations of (b) POC, (c) O_2, and (d) NH_4; (e) bottom water effective remineralization rate; (f) sediment oxygen consumption; and (g) sediment ammonium production for 1–30 June 2006. Model estimates of concentrations and rates were calculated for locations 1 m above the bed, for the inner shelf to midshelf region defined in Figure 1c for both the standard (black lines) and no-resuspension (red lines) model runs. Shaded areas indicate the 5th–95th percentiles of estimates; the thick lines indicate the median values.

O_2 m^{-3} d^{-1} during the small events in 1–23 July 2006 resuspension events (Figures 5e and 6e). This resuspension-induced modification of biogeochemical dynamics decreased median oxygen concentrations by up to ~20 and 7 mmol O_2 m^{-3} during these two time periods, respectively (Figures 5c and 6c). Similarly, median ammonium concentrations increased by about 3 and 1 mmol N m^{-3} during the June 2006 event and periods of resuspension in 1–23 July 2006, respectively (Figures 5d and 6d).

3.2.1. Across-Shelf Variability

Consistent with the time series results presented above, local resuspension-induced changes in bottom water oxygen and ammonium dynamics were generally co-located with increases in POC concentrations in the standard model run results, as illustrated by across-shelf transects for a location west of Atchafalaya Bay (Figure 7). During the June 2006 event, for example, POC concentrations increased throughout the water column in water depths of ~5 m and within the bottom couple meters of the water column in areas 20–40 m deep (Figures 7b and 7c), compared to pre-event and post-event conditions (Figures 7a, 7d, and 7e). Near-bed bottom water oxygen consumption also varied across the shelf, but higher consumption was estimated when and where POC concentrations were high (Figures 7a–7j). A comparison of results of the standard model run and the no-resuspension sensitivity test demonstrated that resuspension caused near-bed oxygen concentrations to decrease by 50–80 mmol O_2 m^{-3} during this 2-week event when and where POC concentrations increased (Figures 7k–7m). Near-bed oxygen concentrations then remained depressed for several days following the event (Figures 7n–7o). In contrast to near-bed dynamics, resuspension-induced changes in upper water column oxygen concentrations were almost zero, except in water depths of ~5 m. A similar analysis of ammonium dynamics indicated that regions with high POC concentrations also had high rates of near-bed ammonium production and increased resuspension-induced ammonium concentrations in the bottom water column during the June 2006 event (results not shown).
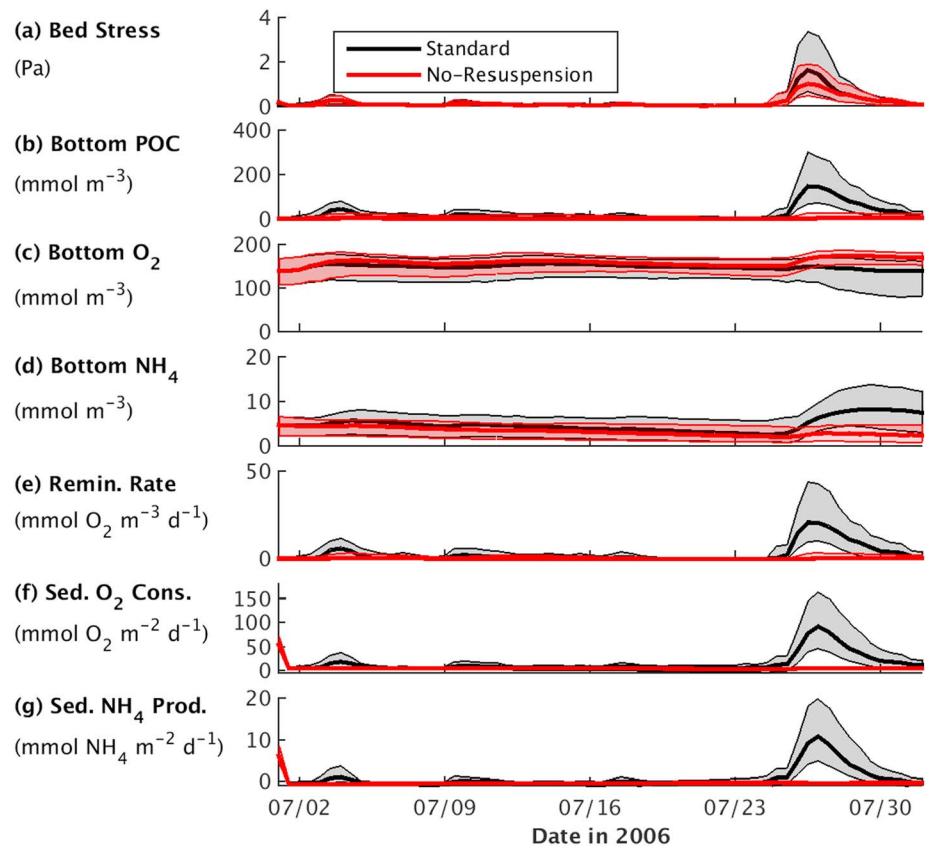
**Figure 6.** Same as above figure, but for 1–31 July 2006.

3.3. Time-Averaged Effects of Resuspension

In addition to causing episodic variability over timescales of hours to days, the effects of cycles of erosion and deposition on biogeochemical dynamics in the standard model run results were evident when results were averaged over month-long time periods. As an example, we present results averaged over 1–30 June 2006, a month in which bed stresses were capable of resuspending sediments over 30% of the time in most regions with water depths of 0–20 m (see Figure 4b). All numbers presented here are means ± standard error and were averaged over the shelf region.

In June 2006, cycles of erosion and deposition increased the effective remineralization rate in the bottom meter of the water column from 1 ± 0.2 mmol O_2 m^{-3} d^{-1} in the no-resuspension model run to 5 ± 1 mmol O_2 m^{-3} d^{-1} in the standard model run (Figure 8a). For the same month, accounting for resuspension in the model decreased average oxygen concentrations in the bottom meter of the water column by ~10 ± 5 mmol O_2 m^{-3} and increased average ammonium concentrations by ~2 ± 0.5 mmol N m^{-3} (Figures 8c and 8d). Consistent with the changes in oxygen concentration, the hypoxic area nearly doubled between the no resuspension model run ($3,000 \pm 300$ km^3) and the standard model run ($6,000 \pm 200$ km^3) in June 2006 (Figure 8b).

The result that remineralization of resuspended seabed organic matter increased oxygen consumption and ammonium production was further investigated using sensitivity tests that examined the effect of altering POM settling velocity and remineralization rate constants. For example, increasing POM settling velocity by a factor of 5 decreased the residence time of resuspended POM in the water column. This reduced remineralization in the fast-settling simulation compared to the standard model run and oxygen and ammonium concentrations were changed by about $+9 \pm 5$ mmol O_2 m^{-3} and -1 ± 0.5 mmol N m^{-3}, respectively, when averaged over the shelf regions in June 2006 (Figure 8). Likewise, decreasing the settling velocities by a factor of 5 increased remineralization, changing oxygen and ammonium concentrations by about -35 ± 6 mmol O_2
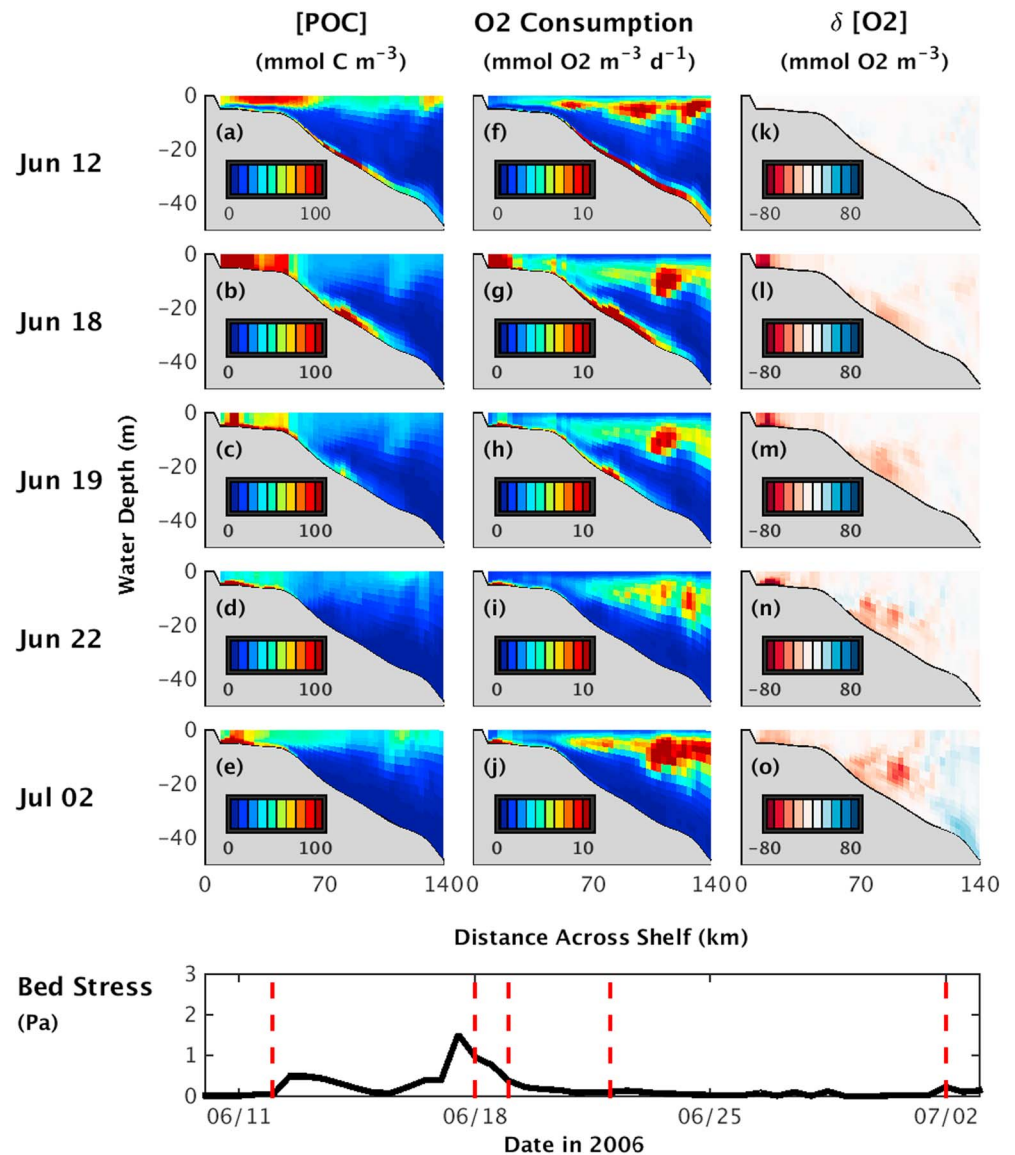
Figure 7. Estimates for a transect west of Atchafalaya Bay (location given in Figure 1). (a–e) POC concentrations (mmol C m^{-3}) from the standard model run. (f–j) Rate of oxygen consumption (mmol O$_2$ m^{-3} d^{-1}) from the standard model run. (k–o) Resuspension-induced changes in oxygen concentration, i.e., oxygen concentration in the standard model run minus values from the no-resuspension simulation (mmol O$_2$ m^{-3}). Each row of panels represents a time before (12 June), during (18–19 June), or after (22 June and 2 July 2) the June resuspension event.

m^{-3} and +6 ± 1 mmol N m^{-3}, respectively, during this time period (Figure 8). Similarly, decreasing (or increasing) the remineralization rate constants reduced (or enhanced) remineralization, in a manner similar to the settling velocity sensitivity tests (Figure 8). Overall, the results from the fast-settling and slow-remineralization sensitivity tests were similar, as, analogously, were estimates from the slow-settling and fast-remineralization sensitivity tests. For all sensitivity tests, the factor of 5 changes in parameters resulted in about a factor of 3 or less change in average effective remineralization rates and concentrations of oxygen and ammonium (Figure 8).

3.3.1. Spatial Variability of Monthly Averaged Results

In addition to the averaged effects on biogeochemical dynamics described above, accounting for resuspension in the standard model run altered spatial gradients in water column biogeochemistry on the northern Gulf of Mexico shelf. Bottom water POC concentrations were largest west of the Mississippi Delta in water
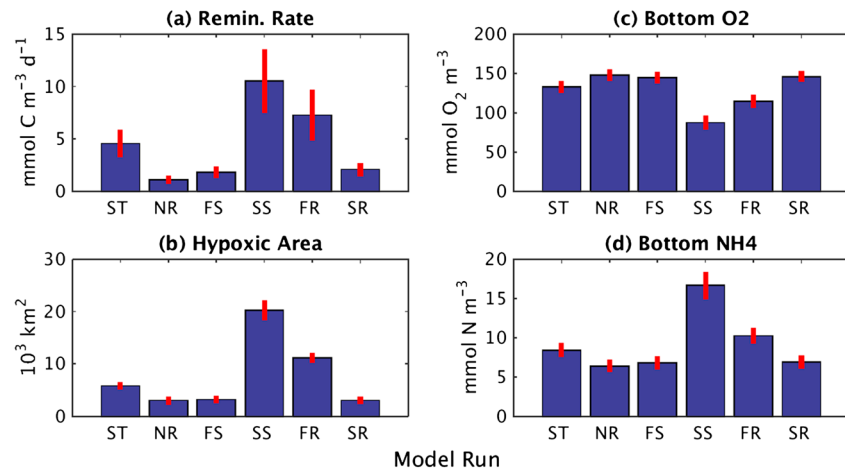
Figure 8. Bar plots of (a) remineralization rate, (b) hypoxic area, (c) O_2 concentration, and (c) NH_4 concentration 1 m above the seabed in the model. Blue bars indicate the mean value; red lines indicate the standard error for each model run. For each plot, estimates are provided for the standard (ST), no-resuspension (NR), fast-settling (FS), slow-settling (SS), fast-remineralization (FR), and slow-remineralization (SR) model runs (see Table 4). All estimates were averaged over June 2006 and the shelf region defined in Figure 1c.

depths up to about 30 m, near the 20-m isobath offshore of Atchafalaya Bay, and in 0–10-m water depths west of Atchafalaya Bay (Figure 9a). This suspended organic matter was generally transported westward away from the Mississippi River Delta and toward the western region of the grid, but variable across-shelf currents diverted some of this material either toward deeper waters or trapped it in eddies (Figure 10a). Comparison of the standard and no-resuspension model runs indicated that without resuspension, bottom water POC concentrations were near zero (Figure 9a). The effect on POC fluxes was variable (Figure 10b), but the largest change was a reduction in the offshore and westward fluxes west of Atchafalaya Bay in 0–10-m water depth. Also, increased transport of POC within the bottom water column both enhanced or reduced depth-integrated fluxes, depending on the direction of baroclinic flows, which altered transport within the eddies west of the Mississippi Delta between −92 and −89.25° longitude (Figure 10b).

POC availability in the bottom water column, modulated by resuspension as described above, was associated with increased remineralization, sediment oxygen consumption, and ammonium production in the standard model run results (Figures 9a, 9b, 9e, and 9f). Both POC concentrations and rates were highest in 0–10-m deep areas west and east of Atchafalaya Bay and between the 20–50-m isobaths between the Mississippi Delta and Atchafalaya Bay. For example, POC concentrations, remineralization, sediment oxygen consumption, and sediment ammonium production varied from low values immediately in front of Atchafalaya Bay and in areas 50–100-m deep to peak values near the 20–50-m isobaths (Figures 9a, 9b, 9e, and 9f). Consistent with these changes, resuspension decreased oxygen concentrations and increased ammonium concentrations in areas with high resuspension-induced POC concentrations, remineralization, sediment oxygen consumption, and sediment ammonium production (Figures 9c and 9d).

### 3.4. Interannual Variability

Estimates from June and July in 2006 and 2007 from the standard model run also demonstrated associations between POC availability and both sediment oxygen consumption and sediment ammonium production (Figure 11). Scatterplots of these two biogeochemical rates versus different environmental variables, including bottom water temperature, oxygen concentration, POC concentration, and bed stress, were examined for model results that were averaged for different spatial regions over summer months in 2006–2007. This analysis indicated that sediment oxygen consumption and ammonium production increased with POC concentration and bed stress for these temporally and spatially averaged model results (Figure 11). Sediment oxygen consumption and ammonium production also decreased with bottom water concentrations of oxygen to a lesser extent and had a weak to negligible relationship with temperature (Figure 11).
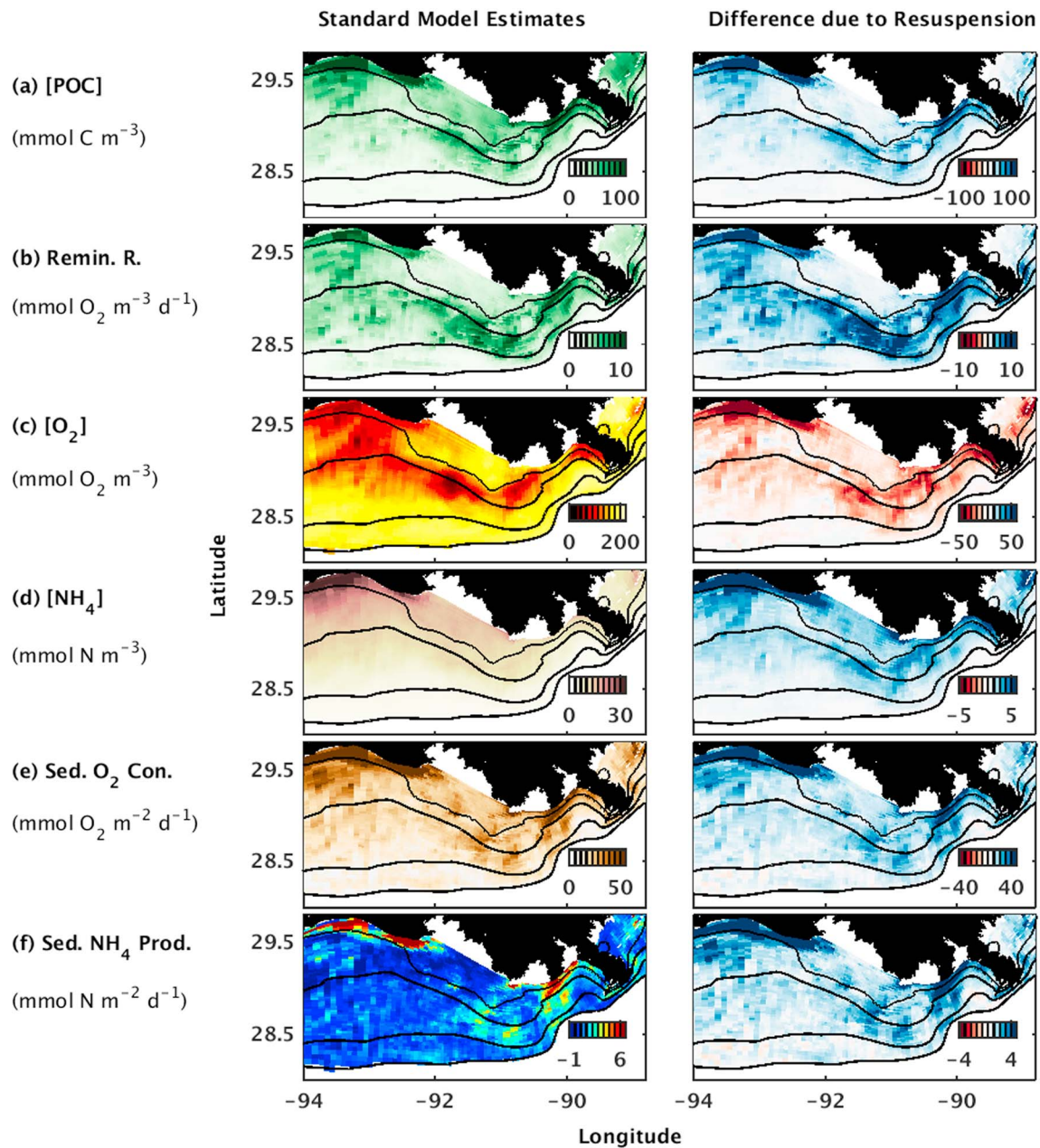
Figure 9. Maps of estimates from the standard model run (left column) and the difference in estimates due to resuspension, calculated as the estimates from the standard model run minus those from the no-resuspension model run (right column), averaged over 1–30 June 2006. Estimates are given for (a) POC concentration (mmol C m^{-3}); (b) effective remineralization rate (Remin. R; mmol O$_2$ m^{-3} d^{-1}); (c) O$_2$ and (d) NH$_4$ concentration (mmol N m^{-3}); (e) sediment oxygen consumption (Sed. O$_2$ Con.; mmol O$_2$ m^{-2} d^{-1}); and (f) sediment ammonium production (Sed. NH$_4$ Con.; mmol N m^{-2} d^{-1}). Estimates of concentration and remineralization were for the locations 1 m above the seabed. Bathymetric contours (black lines) indicate water depths of 10, 20, 50, and 100 m.

4. Discussion

Model estimates indicated that resuspended POM would increase remineralization, as well as sediment oxygen consumption and sediment ammonium production, which would decrease oxygen concentrations and increase ammonium concentrations in the bottom water column. These results were consistent with previous observational (e.g., Aller, 1998; Sloth et al., 1996; Ståhlberg et al., 2006; Tengberg et al., 2003) and modeling studies (Capet et al., 2016; Wainright & Hopkinson, 1997), although the response of nitrogen dynamics to resuspension varies among different systems (e.g., Almroth et al., 2009). Utilizing a three-dimensional coupled sediment transport and biogeochemical model allowed us to build on these previous studies by
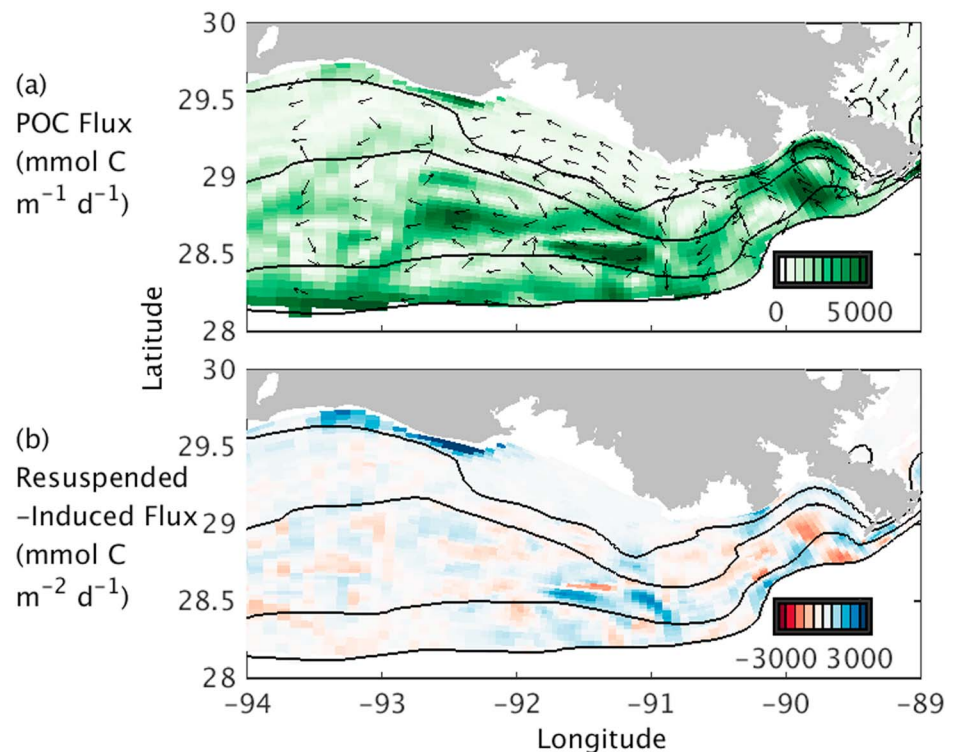
Figure 10. Depth-integrated horizontal POC fluxes averaged over 1–30 June 2006. (a) Magnitude (shading) and direction (arrows) of total fluxes. (b) Resuspended-induced flux, calculated as the difference in flux magnitude between the standard and no-resuspension model runs. Bathymetric contours (black lines) indicate water depths of 10, 20, 50, and 100 m.

examining the spatial and temporal variability of different processes due to environmental factors including resuspension, circulation, temperature, POC availability, and oxygen levels. The following sections synthesize our results in the context of previous research in the northern Gulf of Mexico (section 4.1) and consider implications for future studies and other coastal regions (section 4.2).

4.1. Effect of Resuspension on Remineralization, Oxygen, and Ammonium in the Northern Gulf of Mexico

POM availability in different areas of the shelf was the primary driver of spatial variability in resuspension-induced changes to water column biogeochemistry in the model. POM delivered by the river and produced on the shelf was primarily transported westward along the shelf, with smaller across-shore fluxes (Figure 10). This result contrasts with previous model estimates of inorganic sediment transport from Xu et al. (2011), which showed some large fluxes directed offshore, away from the Mississippi and Atchafalaya river mouths. This difference may be attributed to fact that the Xu et al. (2011) study considered a flood-storm event, while our study period focused on the relatively quiescent summers of 2006 and 2007. Additionally, compared to inorganic sediment, which is sourced to the water column by rivers and seabed resuspension, POM is also derived from shelf water column processes, including photosynthesis and plankton blooms. POM also sinks slowly relative to inorganic sediments. This difference in source and settling velocity would cause POM to remain suspended in westward flowing surface currents on the inner shelf and midshelf for a longer period of time compared to inorganic sediment and implies that export from river mouths would comprise a smaller portion of the POM fluxes than would be expected based on inorganic sediment fluxes.

Our results indicate that remineralization of resuspended and redistributed POM, in addition to seabed respiration, could help explain the spatial patterns of water column biogeochemistry on this shelf. Resuspension-induced increases in POC concentrations were co-located with enhanced effective remineralization rates, lowering oxygen levels in these regions in the model (Figures 9a–9c). In the context of Rowe and Chapman's (2002) conceptual framework, regions of high bottom water POC concentrations in the model
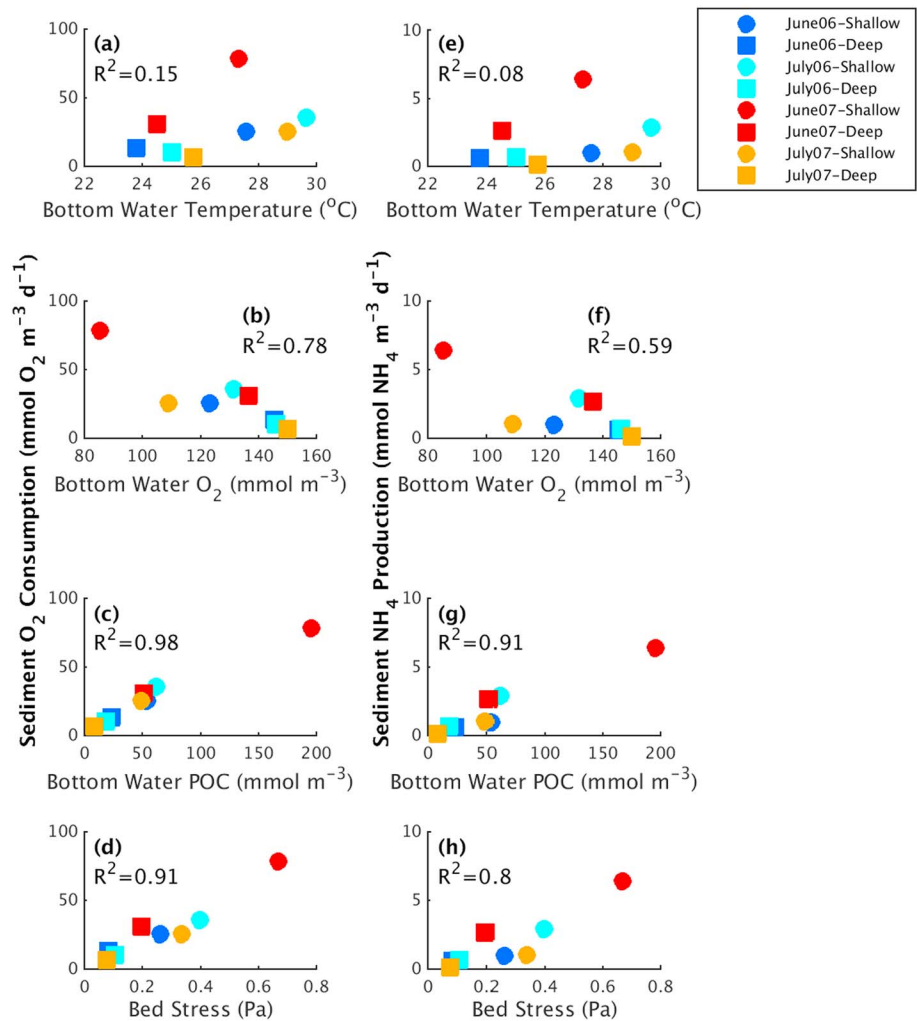
Figure 11. Sediment oxygen consumption (a–d) and sediment ammonium production (e–h) plotted versus (a and e) bottom water temperature, (b and f) oxygen, (c and g) POC, and (d and h) bed stress. Temperature and concentrations were estimated 1 m above the seabed. Each data point represents model averages for one of the spatial domains in Figure 1c and 1 month in 2006–2007, as indicated by the legend.

were similar in location to the Green Water zone, where hypoxia is controlled by organic matter availability and stratification, and the Blue Water zone, where advection of low-oxygen waters and remineralization of organic matter drive hypoxia. Our results extend Rowe and Chapman's conceptual framework by showing that resuspension, in addition to river plume transport, contributes to the along-shelf transport of POM from Brown Water to Green Water to Blue Water zones, affecting the magnitude and location of hypoxia in these downstream regions. Overall, accounting for resuspension in the model doubled hypoxic area from 3,000 to 6,000 km^3 in June 2006 (Figure 8b). This implies that variations in bed stress, currents, and resulting patterns of POM availability could help explain the interannual variability in the location of hypoxia observed in regions west of Atchafalaya Bay (Rabalais et al., 2002).

Resuspension affected oxygen concentrations in a similar manner across the study site in the model but had a greater effect on the aerial extent of hypoxia on the western region of the shelf. When resuspension was neglected in the coupled model, the areal extent of hypoxia decreased more in the western region of the shelf compared to areas immediately west of Mississippi Delta, consistent with previous modeling results indicating that the western portion of the shelf is more sensitive to seabed oxygen consumption compared to other regions (Hetland & DiMarco, 2008; Fennel et al., 2013; Yu, Fennel, & Laurent, 2015). The response of bottom water oxygen concentrations to resuspension, in contrast, was similar along the entire shelf in the

coupled model results; specifically, regions with similar concentrations of POC experienced similar changes in oxygen concentration, despite changes in oxygen availability that modulated effective remineralization rates (Figures 9 and 11). Note that the slope and correlation of this relationship between POC availability and oxygen consumption somewhat depended on the model's use of identical remineralization rate constants for all suspended POM except small detritus and may vary if different parameters were used in the model. Yet the similar response of bottom water oxygen concentrations along different regions of the shelf demonstrates that resuspension plays a consistent role in regulating near-bed biogeochemical dynamics, whereas the relative importance of resuspension, stratification, and other environmental factors for the formation of hypoxia may vary spatially.

The coupled model results similarly support the hypothesis that resuspension could enhance the across-shelf transport of POM produced on the shelf, which affects spatial patterns of hypoxia. Previously published hypotheses suggest that offshore transport of POM from the inner shelf to midshelf could help fuel hypoxia on the midshelf, based on observations of POM concentrations and oxygen budgets (Fry et al., 2015), as well as modeling studies of inorganic sediment transport (Xu et al., 2011) and hydrodynamics (Marta-Almeida et al., 2013; Schiller et al., 2011). In the coupled model, the largest POC fluxes in June 2006 were directed along shelf, but seaward transport of material from areas west of Atchafalaya Bay and bidirectional transport within eddies also occurred (Figure 10). This result suggests that understanding how POM transport is modulated by circulation, for example, by transporting it across the shelf or by isolating organic matter and forming hypoxic *nuclei* within eddies or midwater column layers (Zhang et al., 2015), may improve our ability to predict the spatial variability of hypoxia. Additionally, as noted above, modeled across-shore transport during our relatively quiescent study period was small compared to estimated particulate fluxes during episodic storms and cold fronts (Goñi et al., 2006, 2007; Kineke et al., 2006; Xu et al., 2011, 2016; Figure 10). This implies that episodic POM transport events, such as hurricanes and cold fronts, may disproportionately affect the across-shelf distribution of POM, as well as oxygen and nutrient concentrations.

In addition to transport patterns, across-shelf spatial gradients in bed stress and vertical mixing modulated the extent to which resuspension affected water column biogeochemistry in the model. In contrast to deeper areas, regions shallower than about 20 m experienced strong wave-induced bed stresses that caused frequent and more intense periods of resuspension (Figure 4). In these shallow areas, where bed stresses were sufficiently strong to resuspend sediment most of the time, persistent mixing between the seabed and bottom boundary layer had a nearly continuous effect on biogeochemical signals in the bottom of the water column. In deeper waters, resuspension persisted for only a few days at a time and so the effects were episodic and less substantial compared to shallower areas (Figures 9 and 11). For example, in the standard model run, effective remineralization rates averaged over June 2006 ranged up to ~10 mmol O_2 m^{-3} d^{-1} in water depths 0–20 m (Figure 9b). When erosion was prevented in the no-resuspension sensitivity test, remineralization was reduced by up to 100% compared to the standard model run (Figure 9b). In contrast, in regions 50–100 m deep, time-averaged rates of remineralization were similar in both the standard and no-resuspension model runs (Figure 9b).

4.2. Implications for Future Studies and Other Coastal Regions

Accounting for the influence of resuspension on bottom water biogeochemistry improved our ability to quantify seabed and near-bed processes, including representation of POC concentrations in the model. Organic matter produced on the shelf via photosynthesis or delivered via river inputs creates a local maximum of POC near the surface, a feature reproduced by many biogeochemical models (e.g., Fennel et al., 2013), including ours (Figure 7). In contrast to many previous models (e.g., Fennel et al., 2011, 2013; Yu, Fennel, Laurent, Murrell, & Lehrter, 2015), however, our coupled model could also account for resuspension of POM, which created a second local maxima of POC near the seabed (Figure 7), consistent with observations of vertical profiles of POC (Fry et al., 2015). This indicates that correctly accounting for POM dynamics in this near-bed region is important for future studies focusing on quantifying carbon budgets in the Gulf of Mexico (Bianchi et al., 2007) and other regions (Hofmann et al., 2011; McKee et al., 2004).

Accounting for resuspension also improved the biogeochemical module's ability to represent oxygen consumption and ammonium production, especially in and near the seabed. Parameterizations used by a previous Gulf of Mexico model implementation that was very similar to our coupled model, but did not account for resuspension, often overestimated seabed oxygen consumption while underestimating water

column oxygen consumption (Yu, Fennel, Laurent, Murrell, & Lehrter, 2015). Their model estimates of seabed oxygen consumption generally ranged from ~30 to 50 mmol O_2 m^{-2} d^{-1}, while observations ranged from ~0 to 50 mmol O_2 m^{-2} d^{-1} (Yu, Fennel, Laurent, Murrell, & Lehrter, 2015, Figure 8, and references therein). By implementing a more process-based representation of the seabed biogeochemistry that depended on biogeochemical rates within the seabed, as well as diffusion across the seabed water interface, our coupled model better represented the range of values observed on the shelf (Table 3). Additionally, the increased rates of bottom water remineralization induced by resuspension can help the model represent the increased concentrations of DIN that have been observed during experimental studies (Fanning et al., 1982). This resuspension-induced remineralization also explains why models that neglect cycles of erosion and deposition may underestimate oxygen consumption in the water column, leading to overestimated oxygen concentrations in the Gulf of Mexico (Yu, Fennel, Laurent, Murrell, & Lehrter, 2015; Laurent et al., 2016) and other coastal environments (e.g., Irby et al., 2016).

The large effect of resuspension on bottom water remineralization (Figures 5, 6, and 8) indicates that future models of the northern Gulf of Mexico should prioritize accounting for the effect of erosion and deposition of POM on water column biogeochemistry. In contrast, resuspension-induced changes in seabed fluxes of oxygen and nitrogen were small, implying that this may be less important for inclusion in numerical models. For example, models that simply include POM storage in the seabed and subsequent erosion (e.g., Capet et al., 2016) may sufficiently represent conditions during many time periods, especially for studies focusing on the midshelf where resuspension-induced changes in seabed-water column fluxes are small. Note, however, that this conclusion is limited to the timeframe of our study, i.e., summer months, when bottom water oxygen concentrations are low and likely limit seabed oxygen fluxes. Seabed fluxes and resuspension-induced modulations of these fluxes may be more important in non-summertime months when oxygen concentrations are higher on the midshelf, similar to results seen in other systems (Glud, 2008; Moriarty et al., 2017; Toussaint et al., 2014). Future work could also explore parameterizations, for example, based on bed stress (Figure 11) or organic matter properties (i.e., remineralization rate constant and settling velocity), to account for the effect of resuspension on bottom water and seabed processes. Such parameterizations are especially helpful for running long model simulations that would otherwise require extensive computational resources and have been used, for example, to estimate oxygen concentrations in the northern Gulf of Mexico (e.g., Fennel et al., 2016; Hetland & DiMarco, 2008; Yu, Fennel, & Laurent, 2015) and other coastal systems (e.g., Scully, 2010, 2016).

Our results also underscored the need to obtain field observations during resuspension events to improve our understanding of bottom boundary layer and seabed processes and their role in water column biogeochemistry, including the development and maintenance of hypoxia. For example, resuspension and remineralization of POM shifted the locus of oxygen consumption from the seabed to the water column in many locations in the northern Gulf of Mexico model, especially in shallow waters where resuspension was persistent. Specifically, while seabed oxygen fluxes increased moderately during resuspension events, water column oxygen consumption grew by an order of magnitude during these times (Figure 9e), consistent with findings from the Rhône subaqueous delta (Moriarty et al., 2017; Toussaint et al., 2014). These results imply that biogeochemical observations within the bottom boundary layer and surficial sediments (e.g., Abril et al., 1999), as well as lab experiments focused on the effects of resuspension (e.g., Fanning et al., 1982; Sloth et al., 1996), may be particularly informative.

Future work should also increase our understanding of POM remineralization and particle transport. Remineralization rate constants and hydrodynamic sediment properties had a large effect on model estimates in both our study (Figure 8) and previous work in various settings (Cerco et al., 2013; Laurent et al., 2016; Liu et al., 2007), but vary over orders of magnitude (e.g. 0.001–32 d^{-1} for remineralization rate constant and 0.1–28 m d^{-1} for settling velocity; Fennel et al., 2006; Patten et al., 1966; Testa et al., 2013; Wainright & Hopkinson, 1997; Yu, Fennel, Laurent, Murrell, & Lehrter, 2015). Yet a continuing challenge is quantitatively relating POM composition (e.g., fraction of POM derived from algal versus terrestrial sources) and environmental conditions (e.g., oxygen concentration, frequency of resuspension, and time since POM production) to the remineralization rate constants required by biogeochemical models. Incubation experiments that observe rates of change of POM concentration in laboratory settings (e.g., Fry et al., 2015), and field studies considering the decomposition rates of different organic matter constituents in various environments (e.g., Arzayus & Canuel, 2004), offer useful approaches for measuring this

constant. Similarly, estimating hydrodynamic properties of POM, such as settling velocity and critical shear stress, remains challenging, but measuring both organic matter concentrations, as well as simultaneously estimating particle settling velocity or seabed erodibility (e.g., Patten et al., 1966; Schaaff et al., 2006) are important for development of reliable model parameterizations for numerical models, such as ours, which account for resuspension and transport of POM.

This study focused primarily on near-bed dynamics, but future work could consider how resuspension-induced changes in oxygen and ammonium availability affect upper water column processes including primary production. Laboratory studies have also shown that tidal resuspension can increase nutrient levels and primary production (Porter et al., 2010). Similarly, previous modeling studies in the northern Gulf of Mexico (Eldridge & Morse, 2008) and elsewhere have indicated that increased nutrient fluxes from the seabed can increase primary production in the water column. In the Gulf of Thailand, for example, decreasing the fraction of organic matter that was buried versus remineralized once it settled to the seabed from 100% to 0–14% increased maximum primary production from about 200 to >700 mg C m^{-2} d^{-1} (Liu et al., 2007). This sensitivity of observed and modeled primary production to seabed and near-bed processes implies that resuspension may also affect rates of production in coastal regions.

Process-based interdisciplinary observational and experimental studies, as well as implementing coupled hydrodynamic-sediment transport-biogeochemical models, would also be useful for better understanding how resuspension affects biogeochemical dynamics for other environmental settings and systems. Future studies could, for example, focus on locations where oxygen concentrations vary with POM supply (e.g., northeast Atlantic shelf; Lampitt et al., 1995), accumulation of POM during winter and spring may facilitate summertime nutrient regeneration and primary production (e.g., Patuxent River estuary; Kemp & Boynton, 1984), resuspension of particulates increases light attenuation (e.g., Chesapeake Bay; Cerco & Noel, 2013; Moriarty, 2017), or *suboxic, fluidized bed reactors* affect carbon budgets and other biogeochemical processes (e.g., on submerged deltas; Aller, 1998). By combining observational, experimental, and modeling techniques, studies of other shelves and estuaries would improve our understanding of how resuspension affects biogeochemical processes in different types of coastal systems.

5. Conclusions

The role of resuspension on bottom water oxygen and nitrogen dynamics was investigated using a coupled hydrodynamic-sediment transport-biogeochemical model for the northern Gulf of Mexico. Although resuspension altered seabed fluxes and oxidation of reduced chemical species, enhanced remineralization was the primary driver of increased oxygen consumption and ammonium production during resuspension events. Specifically, resuspension entrained POC from the seafloor into the water column, and the model estimated that this increased effective remineralization rates in the bottom water column from ~0.5 to up to ~15 mmol C m^{-3} d^{-1} during the June 2006 event. During individual resuspension events, this changed median oxygen and ammonium concentrations by up to -13% and $+54\%$, respectively, when results were averaged over the inner shelf and midshelf for water depths of 0–50 m. When averaged over 2 months, resuspension decreased oxygen concentrations by 10% and increased ammonium concentrations by 31%. Overall, entrainment of POM into the water column and its subsequent remineralization were sufficient to shift the locus of oxygen consumption and ammonium production in the model from the seabed to the bottom boundary layer.

The effect of resuspension on bottom water oxygen and ammonium dynamics varied spatially in response to POM availability. Resuspension-induced changes in near-bed biogeochemical rates, and bottom water concentrations of oxygen and ammonium, were largest in shallow areas (<10 m deep) west and east of Atchafalaya Bay and between the 20 and 50-m isobaths between the Mississippi Delta and Atchafalaya Bay. These regions were co-located with areas where currents and bed stress patterns caused frequent resuspension and elevated bottom water POC concentrations. By decreasing oxygen concentrations, resuspension-induced increases in effective remineralization rate enlarged the modeled hypoxic area. When resuspension was neglected in the model, estimated hypoxic area for June 2006 was almost halved. This result underscores the sensitivity of water column biogeochemistry, including hypoxia, to seabed and bottom boundary layer processes.

References

Abril, G., Etcheber, H., Le Hir, P., Bassoullet, P., Boutier, B., & Frankignoulle, M. (1999). Oxic/anoxic oscillations and organic carbon mineralization in an estuarine maximum turbidity zone (The Gironde, France). *Limnology & Oceanography*, 44(5), 1,304–1,315. https://doi.org/10.4319/lo.1999.44.5.1304

Aller, R. C. (1994). Bioturbation and remineralization of sedimentary organic matter: Effects of redox oscillation. *Chemical Geology*, 114(3-4), 331–345. https://doi.org/10.1016/0009-2541(94)90062-0

Aller, R. C. (1998). Mobile deltaic and continental shelf muds as suboxic, fluidized bed reactors. *Marine Chemistry*, 61(3-4), 143–155. https://doi.org/10.1016/S0304-4203(98)00024-3

Allison, M. A., Kineke, G. C., Gordon, E. S., & Goñi, M. A. (2000). Development and reworking of a seasonal flood deposit on the inner continental shelf off the Atchafalaya River. *Continental Shelf Research*, 20(16), 2267–2294. https://doi.org/10.1016/S0278-4343(00)00070-4

Almroth, E., Tengberg, A., Andersson, J. H., Pakhomova, S., & Hall, P. O. J. (2009). Effects of resuspension on benthic fluxes of oxygen, nutrients, dissolved inorganic carbon, iron and manganese in the Gulf of Finland, Baltic Sea. *Continental Shelf Research*, 29(5-6), 807–818. https://doi.org/10.1016/j.csr.2008.12.011

Andersen, F. Ø. (1996). Fate of organic carbon added as diatom cells to oxic and anoxic marine sediment microcosms. *Marine Ecology Progress Series*, 134, 225–233. https://doi.org/10.3354/meps134225

Arzayus, K. M., & Canuel, E. A. (2004). Degradation in sediments of the York River estuary: Effects of biological vs. physical mixing. *Geochimica et Cosmochimica Acta*, 69(2), 455–464. https://doi.org/10.1016/j.gca.2004.06.029

Aulenbach, B., Buxton, H., Battaglin, W., & Coupe, R. (2007). Streamflow and nutrient fluxes of the Mississippi-Atchafalaya river basin and subbasins for the period of record through 2005. Open-File Report 2007–1080, US Geological Survey.

Berg, P. & Huettel, M. (2008). Monitoring the seafloor using the noninvasive eddy correlation technique: Integrated benthic exchange dynamics. *Oceanography*, 21(4), 164–167.

Bianchi, T. S., DiMarco, S. F., Cowan, J. H., Hetland, R. D., Chapman, P., Day, J. W., & Allison, M. A. (2010). The science of hypoxia in the northern Gulf of Mexico: A review. *Science of the Total Environment*, 408(7), 1471–1484. https://doi.org/10.1016/j.scitotenv.2009.11.047

Bianchi, T. S., Galler, J. J., & Allison, M. A. (2007). Hydrodynamic sorting and transport of terrestraily derived organic carbon in sediments of the Mississippi and Atchafalaya Rivers. *Estuarine, Coastal and Shelf Science*, 73(1-2), 211–222. https://doi.org/10.1016/j.ecss.2007.01.004

Boudreau, B. P., & Jorgensen, B. B. (2001). *The benthic boundary layer: Transport processes and biogeochemistry*. New York: Oxford University Press.

Boyer, T. P., Antonov, J. I., Garcia, H. E., Johnson, D. R., Locarnini, R. A., Mishonov, A. V., et al. (2006). World Ocean Database 2005. In S. Levitus (Ed.), *NOAA Atlas NESDIS 60*, (p. 190). Washington, DC, DVDs: US government printing office.

Capet, A., Meysman, F. J. R., Akoumianaki, I., Soetaert, K., & Grégoire, M. (2016). Integrating sediment biogeochemistry into 3D oceanic models: A study of benthic-pelagic coupling in the Black Sea. *Ocean Modelling*, 101, 83–100. https://doi.org/10.1016/j.ocemod.2016.03.006

Caradec, S., Grossi, V., Gilbert, F., Guigue, C., & Goutx, M. (2004). Influence of various redox conditions on the degradation of microalgal triacylglycerols and fatty acids in marine sediments. *Organic Geochemistry*, 35(3), 277–287. https://doi.org/10.1016/j.orggeochem.2003.11.006

Cerco, C. F., Kim, S.-C., & Noel, M. R. (2013). Management modeling of suspended solids in the Chesapeake Bay, USA. *Estuarine, Coastal and Shelf Science*, 116, 87–98. https://doi.org/10.1016/j.ecss.2012.07.009

Cerco, C. F., & Noel, M. R. (2013). Twenty-one-year simulation of Chesapeake Bay water quality using the CE-QUAL-ICM eutrophication model. *Journal of the American Water Resources Association*, 49, 1119–1133. https://doi.org/10.1111/jawr.12107

Chapman, D. C. (1985). Numerical treatment of cross-shelf open boundaries in a Barotropic Coastal Ocean Model. *Journal of Physical Oceanography*, 15(8), 1060–1075. https://doi.org/10.1175/1520-0485(1985)015<1060:NTOCSO>2.0.CO;2

Christiansen, C., Gertz, F., Laima, M. J. C., Lund-Hansen, L. C., Vang, T., & Jürgensen, C. (1997). Nutrient (P, N) dynamics in the Southwestern Kattegat, Scandinavia: Sedimentation and resuspension effects. *Environmental Geology*, 29(1-2), 66–77. https://doi.org/10.1007/s002540050105

Cloern, J. E. (1987). Turbidity as a control on phytoplankton biomass and productivity in estuaries. *Continental Shelf Research*, 7(11-12), 1367–1381. https://doi.org/10.1016/0278-4343(87)90042-2

Conley, D. J., Biorck, S., Bonsdorff, E., Carstensen, J., Destouni, G., Gustafsson, B. G., et al. (2009). Hypoxia-related processes in the Baltic Sea. *Environmental Science & Technology*, 43.

Connolly, T. P., Hickey, B. M., Geier, S. L., & Cochlan, W. P. (2010). Processes influencing seasonal hypoxia in the northern California Current System. *Journal of Geophysical Research*, 115, C03021. https://doi.org/10.1029/2009JC005283

Corbett, D. R., Mckee, B., & Duncan, D. (2004). An evaluation of mobile mud dynamics in the Mississippi River deltaic region. *Marine Geology*, 209(1-4), 91–112. https://doi.org/10.1016/j.margeo.2004.05.028

Da Silva, A. M., Young-Molling, C. C., & Levitus, S. (1994a). Atlas of Surface Marine Data 1994 Vol. 3. In *Anomalies of fluxes of heat and momentum*, NOAA Atlas NESDIS 8, (Vol. 3). Silver Spring, MD: Natl. Oceanic and Atmos. Admin.

Da Silva, A. M., Young-Molling, C. C., & Levitus, S. (1994b). Atlas of Surface Marine Data 1994 Vol. 4. In *Anomalies of fresh water fluxes*, NOAA Atlas NESDIS 9, (Vol. 4). Silver Spring, MD: Natl. Oceanic and Atmos. Admin.

Dauwe, B., Middelburg, J. J., & Herman, P. M. J. (2001). Effect of oxygen on the degradability of organic matter in subtidal and intertidal sediments of the North Sea. *Marine Ecology Progress Series*, 215, 13–22. https://doi.org/10.3354/meps215013

Devereux, R., Lehrter, J. C., Beddick, D. L. Jr., Yates, D. F., & Jarvis, B. M. (2015). Manganese, iron, and sulfur cycling in Louisiana continental shelf sediments. *Continental Shelf Research*, 99, 46–56. https://doi.org/10.1016/j.csr.201503.008

Draut, A. E., Kineke, G. C., Huh, O. K., Grymes, J. M., Westphal, K. A., & Moeller, C. C. (2005). Coastal mudflat accretion under energetic conditions, Louisiana Chenier Plain Coast, USA. *Marine Geology*, 214(1-3), 27–47. https://doi.org/10.1016/j.margeo.2004.10.033

Eldridge, P. M., & Morse, J. W. (2008). Origins and temporal scales of hypoxia on the Louisiana shelf: Importance of benthic and sub-pycnocline water metabolism. *Marine Chemistry*, 108(3-4), 159–171. https://doi.org/10.1016/j.marchem.2007.11.009

Fanning, K. A., Carder, K. L., & Betzer, P. R. (1982). Sediment resuspension by coastal waters: A potential mechanism for nutrient re-cycling on the ocean's margins. *Deep Sea Research*, 29(8), 953–965. https://doi.org/10.1016/0198-0149(82)90020-6

Feist, T. J., Pauer, J. J., Melendez, W., Lehrter, J. C., DePetro, P. A., Rygwelski, K. R., et al. (2016). Modeling the relative importance of nutrient and carbon loads, boundary fluxes, and sediment fluxes on Gulf of Mexico hypoxia. *Environmental Science & Technology*, 50. acs.Est.6b01684. https://doi.org/10.1021/acs.est.6b01684

Fennel, K., Hetland, R., Feng, Y., & DiMarco, S. (2011). A coupled physical-biological model of the northern Gulf of Mexico shelf: Model description, validation and analysis of phytoplankton variability. *Biogeosciences Discussions*, 8(1), 121–156. https://doi.org/10.5194/bgd-8-121-2011

Fennel, K., Hu, J., Laurent, A., Marta-Almeida, M., & Hetland, R. (2013). Sensitivity of hypoxia predictions for the northern Gulf of Mexico to sediment oxygen consumption and model nesting. *Journal of Geophysical. Research :Oceans*, *118*, 990–1002. https://doi.org/10.1002/jgrc.20077

Fennel, K., Laurent, A., Hetland, R., Justić, D., Ko, D. S., Lehrter, J., et al. (2016). Effects of model physics on hypoxia simulations for the northern Gulf of Mexico: A model intercomparison. *Journal of Geophysical. Research: Oceans*, *121*, 5731–5750. https://doi.org/10.1002/2015JC011577

Fennel, K., Wilkin, J., Levin, J., Moisan, J., O'Reilly, J., & Haidvogel, D. (2006). Nitrogen cycling in the Middle Atlantic Bight: Results from a three-dimensional model and implications for the North Atlantic nitrogen budget. *Global Biogeochemical Cycles*, *20*, GB3007. https://doi.org/10.1029/2005GB002456

Fennel, K., Wilkin, J., Previdi, M., & Najjar, R. (2008). Denitrification effects on air-sea CO_2 flux in the coastal ocean: Simulations for the northwest North Atlantic. *Geophysical Research Letters*, *35*, L24608. https://doi.org/10.1029/2008GL036147

Flather, R. A. (1976). A tidal model of the north-west European continental shelf. In J. C. J. Nihoul (Ed.), *Seventh Liege Colloquium on ocean hydrodynamics: Continental shelf dynamics*, (pp. 141–164). Liege: Univerity of Liege.

Forrest, D. R., Hetland, R. D., & DiMarco, S. F. (2012). Corrigendum: Multivariable statistical regression models of the areal extent of hypoxia over the Texas–Louisiana continental shelf. *Environmental Research Letters*, *7*(1), 19501. https://doi.org/10.1088/1748-9326/7/1/019501

Fry, B., Justić, D., Riekenberg, P., Swenson, E. M., Turner, R. E., Wang, L., et al. (2015). Carbon dynamics on the Louisiana continental shelf and cross-shelf feeding of hypoxia. *Estuaries and Coasts*, *38*(3), 703–721. https://doi.org/10.1007/s12237-014-9863-9

Gilbert, F., Hulth, S., Grossi, V., & Aller, R. C. (2016). Redox oscillation and benthic nitrogen mineralization within burrowed sediments: An experimental simulation at low frequency. *Journal of Experimental Marine Biology and Ecology*, *482*, 75–84. https://doi.org/10.1016/j.jembe.2016.05.003

Glud, R. N. (2008). Oxygen dynamics of marine sediments. *Marine Biological Research*, *4*(4), 243–289. https://doi.org/10.1080/17451000801888726

Goñi, M. A., Alleau, Y., Corbett, R., Walsh, J. P., Mallinson, D., Allison, M. A., et al. (2007). The effects of Hurricanes Katrina and Rita on the seabed on the Louisiana shelf. *The Sedimentary Record*, *5*(1), 4–9. https://doi.org/10.2110/sedred.2007.1.4

Goñi, M. A., Gordon, E. S., Monacci, N. M., Clinton, R., Gisewhite, R., Allison, M. A., & Kineke, G. (2006). The effect of Hurricane Lili on the distribution of organic matter along the inner Louisiana shelf (Gulf of Mexico, USA). *Continental Shelf Research*, *26*(17-18), 2260–2280. https://doi.org/10.1016/j.csr.2006.07.017

Grant, W. D., & Madsen, O. S. (1986). The continental-shelf bottom boundary layer. *Annual Review of Fluid Mechanics*, *18*(1), 265–305. https://doi.org/10.1146/annurev.fl.18.010186.001405

Haidvogel, D. B., Arango, H., Budgell, W. P., Cornuelle, B. D., Curchitser, E., Di Lorenzo, E., et al. (2008). Ocean forecasting in terrain-following coordinates: Formulation and skill assessment of the Regional Ocean Modeling System. *Journal of Computational Physics*, *227*(7), 3595–3624. https://doi.org/10.1016/j.jcp.2007.06.016

Haidvogel, D. B., Arango, H. G., Hedstrom, K., Beckmann, A., Malanotte-Rizzoli, P., & Shchepetkin, A. F. (2000). Model evaluation experiments in the North Atlantic Basin: Simulations in nonlinear terrain-following coordinates. *Dynamics of Atmospheres and Oceans*, *32*(3-4), 239–281. https://doi.org/10.1016/S0377-0265(00)00049-X

Hartnett, H. E., Keil, R. G., Hedges, J. I., & Devol, A. H. (1998). Influence of oxygen exposure time on organic carbon preservation in continental margin sediments. *Nature*, *391*(6667), 572–575. https://doi.org/10.1038/35351

Hetland, R. D., & DiMarco, S. F. (2008). How does the character of oxygen demand control the structure of hypoxia on the Texas–Louisiana continental shelf? *Journal of Marine Systems*, *70*(1-2), 49–62. https://doi.org/10.1016/j.jmarsys.2007.03.002

Hetland, R. D., & DiMarco, S. F. (2012). Skill assessment of a hydrodynamic model of circulation over the Texas–Louisiana continental shelf. *Ocean Modelling*, *43-44*, 64–76. https://doi.org/10.1016/j.ocemod.2011.11.009

Hofmann, E. E., Cahill, B., Fennel, K., Friedrichs, M. A. M., Hyde, K., Lee, C., et al. (2011). Modeling the dynamics of continental shelf carbon. *Annual Review of Marine Science*, *3*(1), 93–122. https://doi.org/10.1146/annurev-marine-120709-142740

Irby, I., Friedrichs, M. A. M., Friedrichs, C. T., Bever, A. J., Hood, R. R., Lanerolle, L. W. J., et al. (2016). Challenges associated with modeling low-oxygen waters in Chesapeake Bay: A multiple model comparison. *Biogeosciences*, *13*. https://doi.org/10.5194/bg-13-2011-2016

Justić, D., & Wang, L. (2014). Assessing temporal and spatial variability of hypoxia over the inner Louisiana-upper Texas shelf: Application of an unstructured-grid three-dimensional coupled hydrodynamic-water quality model. *Continental Shelf Research*, *72*, 163–179. https://doi.org/10.1016/j.csr.2013.08.006

Kemp, W., & Boynton, W. (1984). Spatial and temporal coupling of nutrient inputs to estuarine primary production: The role of particulate transport and decomposition. *Bulletin of Marine Science*, *35*(3), 522–535.

Kemp, W., Boynton, W., Adolf, J., Boesch, D., Boicourt, W., Brush, G., et al. (2005). Eutrophication of Chesapeake Bay: Historical trends and ecological interactions. *Marine Ecology Progress Series*, *303*, 1–29. https://doi.org/10.3354/meps303001

Kemp, W. M., Testa, J. M., Conley, D. J., Gilbert, D., & Hagy, J. D. (2009). Temporal responses of coastal hypoxia to nutrient loading and physical controls. *Biogeosciences*, *6*(12), 2985–3008. https://doi.org/10.5194/bg-6-2985-2009

Kineke, G. C., Higgins, E. E., Hart, K., & Velasco, D. (2006). Fine-sediment transport associated with cold-front passages on the shallow shelf, Gulf of Mexico. *Continental Shelf Research*, *26*(17-18), 2073–2091. https://doi.org/10.1016/j.csr.2006.07.023

Lampitt, R. S., Raine, R. C. T., Billett, D. S. M., & Rice, A. L. (1995). Material supply to the European continental slope: A budget based on benthic oxygen demand and organic supply. *Deep Sea Research Part I*, *42*(11-12), 1865–1880. https://doi.org/10.1016/0967-0637(95)00084-4

Laurent, A., Fennel, K., Cai, W.-J., Huang, W.-J., Barbero, L., & Wanninkhof, R. (2017). Eutrophication- induced acidification of coastal waters in the northern Gulf of Mexico: Insights into origin and processes from a coupled physical-biogeochemical model. *Geophysical Research Letters*, *44*, 946–956. https://doi.org/10.1002/2016GL071881

Laurent, A., Fennel, K., Wilson, R., Lehrter, J., & Devereux, R. (2016). Parameterization of biogeochemical sediment–water fluxes using in situ measurements and a diagenetic model. *Biogeosciences*, *13*(1), 77–94. https://doi.org/10.5194/bg-13-77-2016

Lehrter, J. C., Beddick, D. L. Jr., Devereux, R., Yates, D. F., & Murrell, M. C. (2012). Sediment-water fluxes of dissolved inorganic carbon, O_2, nutrients, and N_2 from the hypoxic region of the Louisiana continental shelf. *Biogeochemistry*, *109*(1-3), 233–252. https://doi.org/10.1007/s10533-011-9623-x

Liu, K. K., Chen, Y. J., Tseng, C. M., Lin, I. I., Liu, H. B., & Snidvongs, A. (2007). The significance of phytoplankton photo-adaptation and benthic-pelagic coupling to primary production in the South China Sea: Observations and numerical investigations. *Deep Sea Research Part II Topical Studies in Oceanography*, *54*(14-15), 1546–1574. https://doi.org/10.1016/j.dsr2.2007.05.009

Madsen, O. S. (1994). Spectral wave-current bottom boundary layer flows. *Coastal Engineering*, 384–398.

Marchesiello, P., McWilliams, J. C., & Shchepetkin, A. (2001). Open boundary conditions for long-term integration of regional oceanic models. *Ocean Modelling*, *3*(1-2), 1–20. https://doi.org/10.1016/S1463-5003(00)00013-5

Marta-Almeida, M., Hetland, R. D., & Zhang, X. (2013). Evaluation of model nesting performance on the Texas-Louisiana continental shelf. *Journal of Geophysical Research: Oceans*, *118*, 2476–2491. https://doi.org/10.1002/jgrc.20163

McCarthy, M. J., Carini, S. A., Liu, Z., Ostrom, N. E., & Gardner, W. S. (2013). Oxygen consumption in the water column and sediments of the northern Gulf of Mexico hypoxic zone. *Estuary Coastal and Shelf Science*, *123*, 46–53. https://doi.org/10.1016/j.ecss.2013.02.019

McCarthy, M. J., Newell, S. E., Carini, S. A., & Gardner, W. S. (2015). Denitrification dominates sediment nitrogen removal and is enhanced by bottom-water hypoxia in the northern Gulf of Mexico. *Estuaries and Coasts*, *38*(6), 2279–2294. https://doi.org/10.1007/s12237-015-9964-0

McKee, B. A., Aller, R. C., Allison, M. A., Bianchi, T. S., & Kineke, G. C. (2004). Transport and transformation of dissolved and particulate materials on continental margins influenced by major rivers: Benthic boundary layer and seabed processes. *Continental Shelf Research*, *24*(7-8), 899–926. https://doi.org/10.1016/j.csr.2004.02.009

Moriarty, J. M. (2017). The role of seabed resuspension on oxygen and nutrient dynamics in coastal systems: A numerical modeling study. PhD Dissertation. Virginia Institute of Marine Science, The College of William & Mary. https://doi.org/10.21220/V5RT6R

Moriarty, J. M., Harris, C. K., Fennel, K., Friedrichs, M. A. M., Xu, K., & Rabouille, C. (2017). The roles of resuspension, diffusion and biogeo-chemical processes on oxygen dynamics offshore of the Rhône River, France: A numerical modeling study. *Biogeosciences*, *14*(7), 1919–1946. https://doi.org/10.5194/bg-14-1919-2017

Moriarty, J. M., Harris, C. K., Friedrichs, M. A. M., Fennel, K., & Xu, K. (2018). A model archive for a coupled hydrodynamic-sediment transport-biogeochemistry model for the northern Gulf of Mexico, USA, Virginia Institute of Marine Science, College of William and Mary. https://doi.org/10.21220/rb78-k115.

Murrell, M. C., & Lehrter, J. C. (2011). Sediment and lower water column oxygen consumption in the seasonally hypoxic region of the Louisiana Continental Shelf. *Estuaries and Coasts*, *34*(5), 912–924. https://doi.org/10.1007/s12237-010-9351-9

Murrell, M. C., Stanley, R. S., Lehrter, J. C., & Hagy, J. D. III (2013). Plankton community respiration, net ecosystem metabolism, and oxygen dynamics on the Louisiana continental shelf: Implications for hypoxia. *Continental Shelf Research*, *52*, 27–38. https://doi.org/10.1016/j.csr.2012.10.010

Nielsen, P. (1992). *Coastal bottom boundary layers and sediment transport*. Singapore: World Scientific Publishing Co., Pte. Ltd. https://doi.org/10.1142/1269

Patten, B. C., Young, D. K., & Roberts, M. H. Jr. (1966). Vertical distribution and sinking characteristics of seston in the lower York River, Virginia. *Chesapeake Science*, *7*(1), 20–29. https://doi.org/10.2307/1350985

Porter, E. T., Mason, R. P., & Sanford, L. P. (2010). Effect of tidal resuspension on benthic-pelagic coupling in an experimental ecosystem study. *Marine Ecological Progress Series*, *413*, 33–53. https://doi.org/10.3354/meps08709

Rabalais, N. N., Turner, R. E., & Wiseman, W. J. (2002). Gulf of Mexico Hypoxia, a.k.a. "the Dead Zone." *Annual Review of Ecological Systems*, *33*, 235–263. https://doi.org/10.1146/annurev.ecolsys.33.010802.150513, 1

Rowe, G. T., & Chapman, P. (2002). Continental shelf hypoxia: Some nagging questions. *Gulf of Mexico Science*, *2*, 155–160.

Rowe, G. T., Kaegi, M. E. C., Morse, J. W., Boland, G. S., & Briones, E. G. E. (2002). Sediment community metabolism associated with continental shelf hypoxia, northern Gulf of Mexico. *Estuaries*, *25*(6), 1097–1106. https://doi.org/10.1007/BF02692207

Salisbury, J. E., Campbell, J. W., Linder, E., David Meeker, L., Müller-Karger, F. E., & Vörösmarty, C. J. (2004). On the seasonal correlation of surface particle fields with wind stress and Mississippi discharge in the northern Gulf of Mexico. *Deep Sea Research Part II Topical Studies in Oceanography*, *51*(10-11), 1187–1203. https://doi.org/10.1016/j.dsr2.2004.03.002

Schaaff, E., Grenz, C., Pinazo, C., & Lansard, B. (2006). Field and laboratory measurements of sediment erodibility: A comparison. *Journal of Sea Research*, *55*(1), 30–42. https://doi.org/10.1016/j.seares.2005.09.004

Schiller, R. V., Kourafalou, V. H., Hogan, P., & Walker, N. D. (2011). The dynamics of the Mississippi River plume: Impact of topography, wind and offshore forcing on the fate of plume waters. *Journal of Geophysical Research*, *116*, C06029. https://doi.org/10.1029/2010JC006883

Scully, M. E. (2010). Wind modulation of dissolved oxygen in Chesapeake Bay. *Estuaries and Coasts*, *33*(5), 1164–1175. https://doi.org/10.1007/s12237-010-9319-9

Scully, M. E. (2016). Contribution of physical processes to inter-annual variations of hypoxia in Chesapeake Bay: A 30-yr modeling study. *Limnology and Oceanography*, *61*, 2243–2260. https://doi.org/10.1002/lno.10372

Shchepetkin, A. F. (2003). A method for computing horizontal pressure-gradient force in an oceanic model with a nonaligned vertical coordinate. *Journal of Geophysical Research*, *108*(C3), 3090. https://doi.org/10.1029/2001JC001047

Shchepetkin, A. F., & McWilliams, J. C. (2009). Correction and commentary for "Ocean forecasting in terrain-following coordinates: Formulation and skill assessment of the regional ocean modeling system" by Haidvogel et al., J. Comp. Phys. 227, pp. 3595–3624. *Journal of Computational Physics*, *228*(24), 8985–9000. https://doi.org/10.1016/j.jcp.2009.09.002

Sherwood, C. R., Aretxabaleta, A., Harris, C. K., Rinehimer, J. P., Verney, R., & Ferre, B. (2018). Cohesive and mixed sediment in the Regional Ocean Modeling System (ROMS v3.6) implemented in the Coupled Ocean Atmosphere WAve Sediment-Transport Modeling System (COAWST r1234). *Geoscientific Model Development*, *11*(5), 1849–1871. https://doi.org/10.5194/gmd-11-1849-2018

Sloth, N. P., Riemann, B., Nielsen, L. P., & Blackburn, T. H. (1996). Resilience of pelagic and benthic microbial communities to sediment resus-pension in a coastal ecosystem, Knebel Vig, Denmark. *Estuary Coastaland Shelf Science*, *42*(4), 405–415. https://doi.org/10.1006/ecss.1996.0027

Soetaert, K., Herman, P. M. J., & Middelburg, J. J. (1996a). A model of early diagenetic processes from the shelf to abyssal depths. *Geochimica et Cosmochimica Acta*, *60*(6), 1019–1040. https://doi.org/10.1016/0016-7037(96)00013-0

Soetaert, K., Herman, P. M. J., & Middelburg, J. J. (1996b). Dynamic response of deep-sea sediments to seasonal variations: A model. *Limnology and Oceanography*, *41*(8), 1651–1668. https://doi.org/10.4319/lo.1996.41.8.1651

Ståhlberg, C., Bastviken, D., Svensson, B. H., & Rahm, L. (2006). Mineralisation of organic matter in coastal sediments at different frequency and duration of resuspension. *Estuary Coastal and Shelf Science*, *70*(1-2), 317–325. https://doi.org/10.1016/j.ecss.2006.06.022

Sun, M.-Y., Aller, R. C., Lee, C., & Wakeham, S. G. (2002). Effects on oxygen and redox oscillation on degradation of cell-associated lipids in surficial marine sediment. *Geochimica et Cosmochimica Acta*, *66*(11), 2003–2012. https://doi.org/10.1016/S0016-7037(02)00830-X

Tengberg, A., Almroth, E., & Hall, P. (2003). Resuspension and its effects on organic carbon recycling and nutrient exchange in coastal sediments: In situ measurements using new experimental technology. *Journal of Experimental Marine Biology and Ecology*, *285-6*, 119–142.

Testa, J. M., Brady, D. C., Di Toro, D. M., Boynton, W. R., Cornwell, J. C., & Kemp, W. M. (2013). Sediment flux modeling: Stimulating nitrogen, phosphorus, and silica cycles. *Estuarine, Coastal and Shelf Science*, *131*, 245–263. https://doi.org/10.1016/j.ecss.2013.06.014

Tolman, H. L., Balasubramaniyan, B., Burroughs, L. D., Chalikov, D. V., Chao, Y. Y., Chen, H. S., & Gerald, V. M. (2002). Development and implementation of wind-generated ocean surface wave models at NCEP. *Weather and Forecasting*, *17*(2), 311–333. https://doi.org/10.1175/1520-0434(2002)017<0311:daiowg>2.0.co;2

Toussaint, F., Rabouille, C., Bombled, B., Abchiche, A., Aouji, O., Buchholtz, G., et al. (2014). A new device to follow temporal variations of oxygen demand in deltaic sediments: The LSCE benthic station. *Limnology and Oceanography: Methods*, *12*(11), 729–741. https://doi.org/10.4319/lom.2014.12.729

Wainright, S. C., & Hopkinson, C. S. (1997). Effects of sediment resuspension on organic matter processing in coastal environments: A simulation model. *Journal of Marine Systems*, *11*(3-4), 353–368. https://doi.org/10.1016/S0924-7963(96)00130-3

Wakeham, S. G., & Canuel, E. A. (2006). Degradation and preservation of organic matter in marine sediments. In *Marine organic matter: Biomarkers, isotopes and DNA. Handbook of environmental chemistry*, (Vol. 2N, pp. 295–321). Berlin, Heidelberg: Springer. https://doi.org/10.1007/698_2_009

Wakeham, S. G., Canuel, E. A., Lerberg, E. J., Mason, P., Sampere, T. P., & Bianchi, T. S. (2009). Partitioning of organic matter in continental margin sediments among density fractions. *Marine Chemistry*, *115*(3-4), 211–225. https://doi.org/10.1016/j.marchem.2009.08.005

Warner, J. C., Sherwood, C. R., Signell, R. P., Harris, C. K., & Arango, H. G. (2008). Development of a three-dimensional, regional, coupled wave, current, and sediment-transport model. *Computational Geosciences*, *34*(10), 1284–1306. https://doi.org/10.1016/j.cageo.2008.02.012

Wiberg, P. L., & Sherwood, C. R. (2008). Calculating wave-generated bottom orbital velocities from surface-wave parameters. *Computational Geosciences*, *34*(10), 1243–1262. https://doi.org/10.1016/j.cageo.2008.02.010

Williams, S. J., Arsenault, M. A., Buczkowski, B. J., Reid, J. A., Flocks, J. G., Kulp, M. A., et al. (2006). Surficial sediment character of the Louisiana offshore Continental Shelf region: A GIS compilation. U. S. Geological Survey Open-File Report 2006–1195. Online at </http://pubs.usgs.gov/of/2006/1195/index.htmS>.

Wiseman, W. J., Rabalais, N. N., Turner, R. E., Dinnel, S. P., & MacNaughton, A. (1997). Seasonal and interannual variability within the Louisiana coastal current: Stratification and hypoxia. *Journal of Marine Systems*, *12*(1-4), 237–248. https://doi.org/10.1016/S0924-7963(96)00100-5

Wright, L. D., & Nittrouer, C. A. (1995). Dispersal of river sediments in coastal seas: Six contrasting cases. *Estuaries*, *18*(3), 494–508. https://doi.org/10.2307/1352367

Wysocki, L. A., Bianchi, T. S., Powell, R. T., & Reuss, N. (2006). Spatial variability in the coupling of organic carbon, nutrients, and phytoplankton pigments in surface waters and sediments of the Mississippi River plume. *Estuary Coastal and Shelf Science*, *69*(1-2), 47–63. https://doi.org/10.1016/j.ecss.2006.03.022

Xu, K., Harris, C. K., Hetland, R. D., & Kaihatu, J. M. (2011). Dispersal of Mississippi and Atchafalaya sediment on the Texas–Louisiana shelf: Model estimates for the year 1993. *Continental Shelf Research*, *31*(15), 1558–1575. https://doi.org/10.1016/j.csr.2011.05.008

Xu, K., Mickey, R. C., Chen, Q., Harris, C. K., Hetland, R. D., Hu, K., & Wang, J. (2016). Shelf sediment transport during hurricanes Katrina and Rita. *Computers &Geosciences*, *90*, 24–39. https://doi.org/10.1016/j.cageo.2015.10.009

Yu, L., Fennel, K., & Laurent, A. (2015). A modeling study of physical controls on hypoxia generation in the northern Gulf of Mexico. *Journal of Geophysical Research: Oceans*, *120*, 2813–2825. https://doi.org/10.1002/2014JC010387

Yu, L., Fennel, K., Laurent, A., Murrell, M. C., & Lehrter, J. C. (2015). Numerical analysis of the primary processes controlling oxygen dynamics on the Louisiana shelf. *Biogeosciences*, *12*(7), 2063–2076. https://doi.org/10.5194/bg-12-2063-2015

Zhang, W., Hetland, R. D., DiMarco, S. F., & Fennel, K. (2015). Processes controlling mid-water column oxygen minima over the Texas-Louisiana Shelf. *Journal of Geophysical Research: Oceans*, *120*, 2800–2812. https://doi.org/10.1002/2014JC010568

Zhang, X., Hetland, R. D., Marta-Almeida, M., & DiMarco, S. F. (2012). A numerical investigation of the Mississippi and Atchafalaya freshwater transport, filling and flushing times on the Texas-Louisiana Shelf. *Journal of Geophysical Research*, *117*, C11009. https://doi.org/10.1029/2012JC008108

Ziervogel, K., Dike, C., Asper, V., Montoya, J., Battles, J., D'souza, N., et al. (2015). Enhanced particle fluxes and heterotrophic bacterial activities in Gulf of Mexico bottom waters following storm-induced sediment resuspension. *Deep Sea Research Part II Topical Studies in Oceanography*, *129*, 77–88. https://doi.org/10.1016/j.dsr2.2015.06.017